

**Chiral perturbation theory for  $K^+ \rightarrow \pi^+\pi^0$  decay in the  
continuum and on the lattice**

MAARTEN F.L. GOLTERMAN<sup>1</sup> AND KA CHUN LEUNG<sup>2</sup>

*Department of Physics  
Washington University  
St. Louis, MO 63130, USA*

ABSTRACT: In this paper we use one-loop chiral perturbation theory in order to compare lattice computations of the  $K^+ \rightarrow \pi^+\pi^0$  decay amplitude with the experimental value. This makes it possible to investigate three systematic effects that plague lattice computations: quenching, finite-volume effects, and the fact that lattice computations have been done at unphysical values of the quark masses and pion external momenta (only this latter effect shows up at tree level). We apply our results to the most recent lattice computation (ref. [1]), and find that all three effects are substantial. We conclude that one-loop corrections in chiral perturbation theory help in explaining the discrepancy between lattice results and the real-world value. We also revisit  $B_K$ , which is closely related to the  $K^+ \rightarrow \pi^+\pi^0$  decay amplitude by chiral symmetry.

---

<sup>1</sup> e-mail: maarten@aapje.wustl.edu

<sup>2</sup> e-mail: leung@hbar.wustl.edu

## 1. Introduction

One of the aims of practitioners of lattice QCD is the accurate computation of QCD weak matrix elements. There are two reasons for this. First, such matrix elements are needed in order to explain the experimental values of certain quantities. A prominent example is the  $\Delta I = 1/2$  rule for nonleptonic kaon decay. Second, precise knowledge of the values of weak matrix elements helps with the determination of less well-known entries in the Cabibbo–Kobayashi–Maskawa matrix. An important example is the kaon B-parameter  $B_K$ , which parametrizes the strength of CP-violation in  $K^0 - \bar{K}^0$  mixing. (For these and various other phenomenological aspects of kaon weak interactions, see ref. [2] and references therein; for the lattice approach, see refs. [3,4,5] and references therein.)

Actual lattice calculations [6,7,8,9,1] are hampered by many systematic errors. Even if the continuum limit is obtained, several important sources of error still remain. Two of these are caused by the use of a finite volume and by the use of the quenched approximation. A third systematic effect typically occurs for matrix elements involving more than two external particles. Taking  $K \rightarrow 2\pi$  decay as an example, the matrix element most easily determined from a numerical computation is that with degenerate quark masses, and with all external particles (both the kaon and the two pions in this case) at rest. This does not correspond to the physical situation, where of course  $m_K > 2m_\pi$ , and each of the final pions has a spatial momentum  $|\mathbf{k}| = \sqrt{\frac{1}{4}m_K^2 - m_\pi^2}$  (in the kaon’s rest frame). This implies that such lattice results will have to be extrapolated to physical values of the quark masses and the external momenta.

All of the above described effects can be studied in chiral perturbation theory (ChPT). Finite-volume effects can be calculated in ChPT following ref. [10], while a quenched formulation of ChPT (“quenched chiral perturbation theory,” or QChPT) was developed in ref. [11,12]. The third systematic effect introduced above can also be investigated in ChPT

by simply calculating both the “unphysical” matrix element (with all external particles at rest) and the “physical” one (with the correct kinematics). The ratio of the two then gives an estimate of the factor needed in order to convert the unphysical matrix element into the physical one. This was done at tree level for the decay  $K^+ \rightarrow \pi^+\pi^0$  in refs. [9,1] (at tree level no finite-volume or quenching effects show up in ChPT). It was found that even with the conversion factor (which also corrects for the fact that the quark masses in numerical computations are different from the physical quark masses), the lattice value of the  $K^+ \rightarrow \pi^+\pi^0$  matrix element is about two times larger than its experimental value.

In this paper we study the  $K^+ \rightarrow \pi^+\pi^0$  weak matrix element and  $B_K$  in ChPT to one-loop order. This is interesting for various reasons. Nontrivial finite-volume and quenching effects show up in ChPT first at one loop, and therefore a one-loop calculation will give us insight into the size of these effects. Also, there are one-loop corrections to the tree-level conversion factor between unphysical and physical  $K^+ \rightarrow \pi^+\pi^0$  matrix elements, and one would like to know whether these corrections can be part of the explanation that numerical results appear to come out too large [4]. Moreover, it has been suggested that one can expect such one-loop effects to be sizeable, since they include an estimate of the effect of final-state interactions of the two pions [13].

We restrict ourselves to  $B_K$  and  $K^+ \rightarrow \pi^+\pi^0$  decay because these two quantities require the introduction of only one new parameter at the lowest order in ChPT. This is because the corresponding weak operators are both components of the same  $SU(3)$ -flavor 27-plet, and this 27-plet has a unique representation in lowest order ChPT. It would of course be interesting to also consider  $K^0 \rightarrow \pi^+\pi^-$  decay, but this would lead to the introduction of new parameters (corresponding to the  $SU(3)$  octet operators that contribute to this decay). Also, it has been observed that inclusion of the  $\sigma$  resonance may be required for a full understanding of this decay on the lattice [14], which would take us outside of the systematic approach of ChPT.

Beyond lowest order in ChPT, a large number of new operators exist which can contribute

to  $B_K$  and to  $K^+ \rightarrow \pi^+\pi^0$  decay [15], each with its accompanying new parameter (the so-called  $O(p^4)$  low-energy constants). The values of these new parameters are largely unknown. Therefore, at one loop we can only estimate the size of the nonanalytic terms (using a reasonable value of the cutoff), because the nonanalytic terms do not depend on these new parameters. In this paper, we will assume that using a reasonable value of the cutoff in the nonanalytic terms and setting the  $O(p^4)$  low-energy constants to zero will lead to a valid estimate of the size of corrections to tree-level ChPT results. Some idea about the quantitative uncertainties introduced by this approach can be obtained from the sensitivity of our results to the value of the cutoff. These issues will all be discussed in more detail in due course in this paper.

Let us end the introduction with an overview of the paper. We revisit  $B_K$  in section 3 (quenching and finite-volume effects for  $B_K$  have been calculated within ChPT before in refs. [12,5]), while the calculations for the  $K^+ \rightarrow \pi^+\pi^0$  matrix element are contained in sections 4–6. In section 3 we also discuss our approach to the use of ChPT at one loop in some more detail. In section 4 we present our calculation of the nonanalytic one-loop corrections for the physical matrix element. Section 5 explains which Euclidean correlation function is computed in numerical lattice QCD, and in section 6 we present in some detail the calculation of this correlation function in one-loop (Q)ChPT. For this calculation we restrict ourselves to the case of degenerate quark masses ( $m_u = m_d = m_s$ ). In section 7, we use the results of the previous sections in order to obtain quantitative estimates of the various systematic effects for typical lattice computations. We start with calculating the size of the nonanalytic one-loop corrections in the real world, as was done before by Bijmans *et al.* in ref. [16] and by various other authors [17,18,19,20]. We then estimate the one-loop correction to the conversion of the unphysical lattice  $K^+ \rightarrow \pi^+\pi^0$  matrix element to the physical one in the unquenched theory. Next, we include the changes that result from using the quenched approximation for the unphysical matrix element, and we discuss the numerical

results of ref. [1]. The uncertainties introduced by our lack of knowledge of all low-energy constants are discussed. We end this section by considering a quantity which is basically the ratio of  $B_K$  and the  $K^+ \rightarrow \pi^+\pi^0$  matrix element [21]. This quantity is interesting because it is independent of the tree-level low-energy constant, and therefore not sensitive to ambiguities in its value. All calculations are repeated for the finite spatial volume which was used in ref. [1]. Our conclusions are in section 8. Section 2 contains a summary of other (Q)ChPT results that we will need in this paper. Appendix A presents an adaptation of the quenched  $B_K$  result relevant to staggered fermion QCD, and Appendix B relates our result for the  $K^+ \rightarrow \pi^+\pi^0$  correlation function to the general analysis of such Euclidean correlation functions in ref. [22]. Appendix C deals with a technicality.

## 2. Essentials of ChPT and QChPT

We start with a summary of results in ChPT [23,24,25] that we will need in this paper. This also gives us an opportunity to establish our notation. We will refer to the theory without quenching as the “full” or “unquenched” theory. The  $SU(3)$ -octet Goldstone meson fields are organized in the nonlinear representation

$$\Sigma = \exp\left(\frac{2i\phi}{f}\right), \quad (1)$$

where  $\phi$  is the hermitian matrix

$$\phi = \begin{pmatrix} \frac{\pi^0}{\sqrt{2}} + \frac{\eta}{\sqrt{6}} & \pi^+ & K^+ \\ \pi^- & -\frac{\pi^0}{\sqrt{2}} + \frac{\eta}{\sqrt{6}} & K^0 \\ K^- & \bar{K}^0 & -\frac{2\eta}{\sqrt{6}} \end{pmatrix}, \quad (2)$$

and  $f$  is a parameter with the dimension of a mass. Masses of the  $u$ ,  $d$  and  $s$  quarks are incorporated in the mass matrix

$$M = \begin{pmatrix} m_u & 0 & 0 \\ 0 & m_d & 0 \\ 0 & 0 & m_s \end{pmatrix}. \quad (3)$$

To lowest order (which we will refer to as  $O(p^2)$ ) in ChPT, the Euclidean Lagrangian is constructed with the introduction of an additional parameter  $v$ :

$$\mathcal{L} = \frac{f^2}{8} \text{Tr} \left( \partial^\mu \Sigma \partial_\mu \Sigma^\dagger \right) - v \text{Tr} \left( M \Sigma^\dagger + M^\dagger \Sigma \right) . \quad (4)$$

One can read off the tree-level meson masses from the quadratic terms, after expanding  $\Sigma$  in  $\phi$  (for simplicity we will choose  $m_u = m_d = m$ ):

$$m_{\pi,0}^2 = \frac{8vm}{f^2} , \quad m_{K,0}^2 = \frac{4v(m+m_s)}{f^2} , \quad m_{\eta,0}^2 = \frac{8v(m+2m_s)}{3f^2} . \quad (5)$$

It follows that

$$m_{\eta,0}^2 = \frac{4}{3} m_{K,0}^2 - \frac{1}{3} m_{\pi,0}^2 , \quad (6)$$

which predicts a value of the  $\eta$ -mass about 3% too large.

At tree level, the parameter  $f$  is the weak decay constant,  $f = f_\pi = f_K$ . At one loop the pion and kaon decay constants  $f_\pi$  and  $f_K$  and corresponding wavefunction renormalizations  $Z_\pi$  and  $Z_K$  are given by

$$f_\pi = f \left( 1 + \frac{m_K^2}{(4\pi f)^2} [I_\pi + K_1 + K_2 y_\pi] \right) , \quad (7)$$

$$Z_\pi = 1 - \frac{2m_K^2}{3(4\pi f)^2} [I_\pi + K_1 + K_2 y_\pi] \quad (8)$$

for the pion and

$$f_K = f \left( 1 + \frac{m_K^2}{(4\pi f)^2} \left[ I_K + \left( \frac{K_1}{2} + K_2 \right) + \frac{K_1}{2} y_\pi \right] \right) , \quad (9)$$

$$Z_K = 1 - \frac{2m_K^2}{3(4\pi f)^2} \left[ I_K + \left( \frac{K_1}{2} + K_2 \right) + \frac{K_1}{2} y_\pi \right] \quad (10)$$

for the kaon, where

$$I_\pi = -\log \frac{m_K^2}{m_\pi^2} - \left( 1 + 2y_\pi \right) \log \frac{m_\pi^2}{\Lambda^2} , \quad (11)$$

$$I_K = -\frac{3}{2} \log \frac{m_K^2}{m_\pi^2} - \left( 1 - \frac{1}{4} y_\pi \right) \log \frac{m_\eta^2}{m_\pi^2} - \frac{1}{2} \left( 5 + y_\pi \right) \log \frac{m_\pi^2}{\Lambda^2} . \quad (12)$$

In these equations, we made use of the fact that we can replace the tree-level quantities  $m_{\pi,0}^2$ ,  $m_{K,0}^2$  and  $m_{\eta,0}^2$  by their renormalized physical values  $m_\pi^2$ ,  $m_K^2$  and  $m_\eta^2$ . The parameter  $y_\pi$  is defined as

$$y_\pi = \frac{m_\pi^2}{m_K^2} . \quad (13)$$

$\Lambda$  is the cutoff, and the dimensionless parameters  $K_1$  and  $K_2$  are contact-term coefficients coming from the  $O(p^4)$  chiral Lagrangian [25].

A Lagrangian formulation of quenched ChPT (QChPT) was developed in ref. [11]. The basic feature is the introduction of (unphysical) spin 1/2 “ghost” quarks with bosonic statistics and the same masses as the physical quarks, so that their virtual quark-loop contributions cancel those from the original quarks [26]. As a result, the  $\eta'$  meson is light [27,11,12], and therefore needs to be kept in the chiral Lagrangian. The original octet Eq. (1) has to be extended into a nonet to include the  $\eta'$ :

$$\Sigma_q = e^{i\eta'/\sqrt{3}f_q} \Sigma , \quad (14)$$

where  $f_q$  is the quenched parameter equivalent to  $f$  in the full theory, and  $f$  is replaced by  $f_q$  in Eq. (1). In the mass-degenerate case  $m_u = m_d = m_s$ , the  $\eta'$  two-point function acquires both single- and double-pole terms:

$$G_{\eta',\eta'}(p, q) \equiv \langle \eta'(p)\eta'(q) \rangle = \delta(p+q) \left( \frac{1}{p^2 + m_{\pi,0}^2} - \frac{\mu^2 + \alpha p^2}{(p^2 + m_{\pi,0}^2)^2} \right) , \quad (15)$$

where  $\mu^2$  is a parameter which would correspond to the singlet part of the  $\eta'$  mass in full QCD. In full QCD, an estimate using the experimental mass of the  $\eta'$  gives:  $\mu^2/3 \approx (500 \text{ MeV})^2$  (for  $\alpha = 0$ ). In the mass-nondegenerate case  $m_u = m_d \neq m_s$ , the  $\eta$  two-point function also acquires a double-pole term through mixing with the  $\eta'$ . It is then simpler to work in the (nondiagonal) basis of  $\bar{u}u$ ,  $\bar{d}d$ , and  $\bar{s}s$  meson states in the neutral sector (labeled by  $i = u, d, s$  respectively). Their two-point functions are:

$$G_{i,j}(p, q) = \delta(p+q) \left( \frac{\delta_{ij}}{p^2 + M_i^2} - \frac{(\mu^2 + \alpha p^2)/3}{(p^2 + M_i^2)(p^2 + M_j^2)} \right) , \quad (16)$$

where  $M_i^2 \equiv 8vm_i/f_q^2$ . When  $m_u = m_d \neq m_s$ , it is easy to see that  $M_u^2 = M_d^2 = m_{\pi,0}^2$  and  $M_s^2 = 2m_{K,0}^2 - m_{\pi,0}^2$ . We define

$$\delta \equiv \frac{\mu^2/3}{8\pi^2 f_q^2} \quad (17)$$

for later use.

The quenched one-loop expressions for the weak decay constants  $f_\pi$  and  $f_K$  and wave-function renormalizations  $Z_\pi$  and  $Z_K$  in the mass-nondegenerate case ( $m_u = m_d \neq m_s$ ) are

$$f_\pi = f_q \left( 1 + \frac{m_\pi^2}{(4\pi f_q)^2} \tilde{K} \right), \quad (18)$$

$$Z_\pi = 1 - \frac{2m_\pi^2}{3(4\pi f_q)^2} \tilde{K}, \quad (19)$$

$$f_K = f_q \left( 1 + \tilde{I}_K + \frac{m_K^2}{(4\pi f_q)^2} \tilde{K} \right), \quad (20)$$

$$Z_K = 1 - \frac{2}{3} \left[ \tilde{I}_K + \frac{m_K^2}{(4\pi f_q)^2} \tilde{K} \right], \quad (21)$$

where

$$\tilde{I}_K = -\frac{1}{2}\delta \left( 1 + \frac{1}{2(1-y_\pi)} \log \left( \frac{y_\pi}{2-y_\pi} \right) \right) + \frac{1}{3}\alpha \frac{m_K^2}{(4\pi f_q)^2} \left( 1 + \frac{y_\pi(2-y_\pi)}{2(1-y_\pi)} \log \left( \frac{y_\pi}{2-y_\pi} \right) \right), \quad (22)$$

and the dimensionless parameter  $\tilde{K}$  is again a contact-term coefficient from the  $O(p^4)$  Lagrangian. In contrast to the full theory, there is only one such coefficient in the quenched case. In ChPT, an  $O(p^4)$  operator containing the trace of the mass matrix  $M$ , Eq. (3), when evaluated at tree level, contributes to a particular linear combination of  $K_1$  and  $K_2$  in the unquenched quantities. However, in QChPT, the same operator is converted into one where the supertrace [11] of the mass matrix, now enlarged to include the ghost-quark masses, is taken, and hence its contribution to Eqs. (18,19,20,21) vanishes. Note that chiral logarithms and  $\delta$  or  $\alpha$  dependence are absent in Eq. (18) and Eq. (19). This is a consequence of taking  $m_u = m_d$ .



In general, the double poles in Eq. (16) lead to severe infra-red divergences in physical quantities in QChPT. In fact, physical quantities with a singular chiral limit and/or anomalous volume dependence were found in refs. [11,12,28,29,30,31,32]. An example is  $f_K$  in Eq. (20), which diverges in the limit  $y_\pi \rightarrow 0$ .

### 3. Review of $B_K$

The kaon B-parameter  $B_K$  is defined as

$$B_K = \frac{\langle \bar{K}^0 | (\bar{s}d\bar{s}d)_{LL} | K^0 \rangle}{\frac{8}{3} f_K^2 m_K^2}, \quad (23)$$

in which the four-quark operator is defined by

$$(\bar{q}_1 q_2 \bar{q}_3 q_4)_{LL} = (\bar{q}_{1L} \gamma^\mu q_{2L}) (\bar{q}_{3L} \gamma_\mu q_{4L}), \quad (24)$$

where  $q_L = \frac{1}{2}(1 - \gamma_5)q$  is a left-handed quark field. The denominator in Eq. (23) is the matrix element  $\langle \bar{K}^0 | (\bar{s}d\bar{s}d)_{LL} | K^0 \rangle$  evaluated by vacuum saturation. In ChPT, weak-interaction operators, the chiral transformation properties of which are dictated by the Standard Model, are constructed from the Goldstone meson field  $\Sigma$  and the mass matrix  $M$ . The operator  $(\bar{s}d\bar{s}d)_{LL}$  is a component of a 27-plet of  $SU(3)_L$  and has  $\Delta S = 2$ . To lowest order in ChPT ( $O(p^2)$ ), there is only one 27-plet operator:

$$O' = \alpha_{27} t_{kl}^{ij} (\Sigma \partial^\mu \Sigma^\dagger)_{ik} (\Sigma \partial_\mu \Sigma^\dagger)_{jl}, \quad (25)$$

where the tensor  $t_{kl}^{ij}$  satisfies:

$$\sum_i t_{ik}^{ij} = 0, \quad \sum_i t_{ki}^{ij} = 0 \quad \text{and} \quad t_{kl}^{ij} = t_{lk}^{ji}. \quad (26)$$

In order to select the  $\Delta S = 2$  component, we set

$$t_{33}^{22} = 1 \quad (27)$$

and all other components to zero. The parameter  $\alpha_{27}$  is not constrained by any symmetry and its value is determined by QCD dynamics. At tree level (or order  $p^2$ ), one obtains

$$\langle \bar{K}^0 | O' | K^0 \rangle = \frac{8\alpha_{27}}{f^2} m_K^2. \quad (28)$$

The factor  $m_K^2$  comes from a factor  $p_K^2$  where we take the external kaon momentum  $p_K$  on shell, *i.e.*  $m_K$  here is the renormalized physical kaon mass. Therefore,

$$B_K^{full} = \frac{3\alpha_{27}}{f^4} \equiv B^f \quad (29)$$

( $f_K = f$  at tree level).

In this paper, we are interested in corrections of order one higher in ChPT power counting [24,25]. We will refer to these as  $O(p^4)$  contributions. In general, they consist of one-loop corrections coming from the  $O(p^2)$  operators along with tree-level contributions from  $O(p^4)$  operators. A large number of  $O(p^4)$  operators with the symmetries of the operator in Eq. (23) can be constructed from  $\Sigma$  and  $M$ ; see ref. [15] for a complete list of  $O(p^4)$  operators that are relevant to strangeness-changing nonleptonic weak-decay processes involving up to four Goldstone mesons. Each of them is associated with an arbitrary coefficient, which, just like  $\alpha_{27}$ , cannot be determined within ChPT. Since at  $O(p^4)$  only tree-level contributions from these operators are needed, contact terms with arbitrary coefficients result. In contrast, one-loop contributions from  $O(p^2)$  operators generically give rise to nonanalytic functions of the quark masses with coefficients determined by the  $O(p^2)$  operators, and a cutoff  $\Lambda$  naturally arises. The dependence on the cutoff of the  $O(p^4)$ -operator coefficients can then be chosen such that physical quantities are independent of the cutoff.

In order to determine the  $O(p^4)$ -operator coefficients, many authors have used combinations of particle phenomenology and theoretical ideas such as large- $N_c$  arguments, resonance-dominance models, etc. (see for instance refs. [17,18,19,20,25,33,34]). A less phenomenological approach is to find relations between different physical quantities that are independent of  $O(p^2)$ - and  $O(p^4)$ -operator coefficients. An illustrative example is the combination

$f_\eta f_\pi^{1/3}/f_K^{4/3}$  of the pion, kaon and eta decay constants [25]; examples in QChPT can be found in refs. [28,35,32]. In this approach, physical predictions at order  $p^4$  are made without the model-dependent uncertainties mentioned above. These relations of course are precisely the Ward-identities associated with spontaneously broken chiral symmetry. Theoretically, an infinite number of such relations can be constructed. However, the large number of low-energy constants at order  $p^4$  makes this difficult in practice. This is certainly true when we only consider  $B_K$  and  $K^+ \rightarrow \pi^+ \pi^0$  decay, both of which depend on a large number of  $O(p^4)$  low-energy constants. (A program to determine some of these coefficients from experiment in the  $m_\pi = 0$  approximation has been carried out in refs. [18,19].) In this paper, we will limit ourselves mainly to the nonanalytic one-loop corrections. With a reasonable choice of the cutoff, the magnitude of the corrections to the tree-level expressions for certain quantities can be estimated.

Next, we present the results for the full and quenched  $K^0 - \bar{K}^0$  matrix elements of the operator  $O'$  to one loop. For the full case, we obtain

$$\begin{aligned} \langle \bar{K}^0 | O' | K^0 \rangle^f = \frac{8\alpha_{27} m_K^2}{f^2} \left( 1 + \frac{m_K^2}{(4\pi f)^2} \left[ I + F_1 + F_2 + F_3 - (F_2 + 2F_3) y_\pi + F_3 y_\pi^2 \right. \right. \\ \left. \left. - \frac{2}{3} \left( \frac{K_1}{2} + K_2 \right) - \frac{K_1}{3} y_\pi \right] \right), \end{aligned} \quad (30)$$

where

$$I = -5 \log \frac{m_K^2}{m_\pi^2} - \frac{1}{6} (4 - y_\pi) (10 - y_\pi) \log \frac{m_\eta^2}{m_\pi^2} - \frac{1}{3} (35 - y_\pi + 2y_\pi^2) \log \frac{m_\pi^2}{\Lambda^2}, \quad (31)$$

while for the quenched case

$$\begin{aligned} \langle \bar{K}^0 | O' | K^0 \rangle^q = \frac{8\alpha_{27}^q m_K^2}{f_q^2} \left( 1 + \frac{m_K^2}{(4\pi f_q)^2} \left[ \tilde{I} + \tilde{F}_1 + \tilde{F}_3 - 2\tilde{F}_3 y_\pi + \tilde{F}_3 y_\pi^2 - \frac{2\tilde{K}}{3} \right] \right. \\ \left. + \delta I_\delta + \frac{2}{3} \alpha \frac{m_K^2}{(4\pi f_q)^2} I_\alpha \right), \end{aligned} \quad (32)$$

where

$$\tilde{I} = -2(4 - 2y_\pi + y_\pi^2) \log \frac{m_K^2}{\Lambda^2} - y_\pi(1 + y_\pi) \log y_\pi - (2 - y_\pi)(3 - y_\pi) \log(2 - y_\pi), \quad (33)$$

$$I_\delta = -3 - \frac{2 + 2y_\pi - y_\pi^2}{2(1 - y_\pi)} \log\left(\frac{y_\pi}{2 - y_\pi}\right), \quad (34)$$

$$I_\alpha = 2(1 - y_\pi)^2 \log\left(\frac{m_\pi^2}{\Lambda^2}\right) - \frac{2 - y_\pi}{2(1 - y_\pi)} (2 - 7y_\pi + 2y_\pi^2) \log\left(\frac{y_\pi}{2 - y_\pi}\right) + 4 - 2y_\pi + y_\pi^2, \quad (35)$$

with  $y_\pi$  defined in Eq. (13) and  $\delta$  in Eq. (17). In QChPT, the operator  $(\bar{s}d\bar{s}d)_{LL}$  is represented by Eq. (25) with  $\alpha_{27}$  replaced by a new parameter  $\alpha_{27}^q$ . The mass relation Eq. (6) has been used to eliminate  $m_\eta$  in favor of  $m_\pi$  and  $m_K$ , except in the  $\eta$  chiral logarithm of Eq. (30). The dimensionless parameters  $F_i$  and  $\tilde{F}_j$  with  $i = 1, 2, 3$  and  $j = 1, 3$  come from  $O(p^4)$  weak operators. They are parametrized in such a way as to obtain simple expressions for  $B_K$  below. There are just two instead of three independent contact-term coefficients in the quenched case: the reason is the same as that for the analogous difference between the full and quenched  $O(p^4)$  expressions for  $f_{\pi,K}$  and  $Z_{\pi,K}$  in the previous section. These results do not include finite-volume corrections, which are exponentially small in  $m_\pi L$  for large volume (where  $L$  is the linear dimension of the spatial volume) [12].

The results for  $B_K$  to one loop for respectively the full and quenched theories in the mass-nondegenerate case are

$$B_K^f = B^f \left( 1 + \frac{m_K^2}{(4\pi f)^2} \left[ - \left( 1 - \frac{3\epsilon}{2} + \frac{\epsilon^2}{2} \right) \log \frac{m_\pi^2}{\Lambda^2} - 2 \log \frac{m_K^2}{\Lambda^2} - 3 \left( 1 + \frac{\epsilon}{2} + \frac{\epsilon^2}{18} \right) \log \frac{m_\eta^2}{\Lambda^2} - \frac{8}{3} (K_1 + K_2) + \frac{4K_1}{3} \epsilon + F_1 + F_2 \epsilon + F_3 \epsilon^2 \right] \right), \quad (36)$$

and

$$B_K^q = B^q \times \left( 1 + \frac{m_K^2}{(4\pi f_q)^2} \left[ -2(3 + \epsilon^2) \log \frac{m_K^2}{\Lambda^2} - (2 + \epsilon^2) \log(1 - \epsilon^2) - 3\epsilon \log \frac{1 + \epsilon}{1 - \epsilon} - \frac{8\tilde{K}}{3} + \tilde{F}_1 + \tilde{F}_3 \epsilon^2 \right] - \delta \left[ -\frac{2 - \epsilon^2}{2\epsilon} \log \frac{1 + \epsilon}{1 - \epsilon} + 2 \right] + \frac{2}{3} \alpha \frac{m_K^2}{(4\pi f_q)^2} \left[ 2\epsilon^2 \log \left( \frac{m_K^2}{\Lambda^2} (1 - \epsilon) \right) - \frac{1 - 2\epsilon^2 - \epsilon^3}{\epsilon} \log \frac{1 + \epsilon}{1 - \epsilon} + 2 + \epsilon^2 \right] \right). \quad (37)$$

The parameter  $\epsilon$  is defined as

$$\epsilon \equiv 1 - \frac{m_\pi^2}{m_K^2} = \frac{m_s - m}{m_s + m} = 1 - y_\pi . \quad (38)$$

(In Appendix A we present a modified expression for  $B_K^q$  which may be applicable when quenched staggered fermions are used at nonzero lattice spacing and flavor symmetry is not fully restored.) The parameter  $B^f$  is defined in Eq. (29), and  $B^q$  is defined from  $\alpha_{27}^q$  and  $f_q$  by an equation similar to Eq. (29). As is clear from these expressions, the full and quenched theories are entirely different theories. In particular, there is no reason to believe that the coefficients of the  $O(p^2)$  and  $O(p^4)$  operators should be the same in ChPT and QChPT. The  $\delta$  and  $\alpha$  terms in Eq. (37) come from the double poles in Eq. (16). The full ChPT result Eq. (36) has previously been calculated in ref. [16] in the  $m_\pi = 0$  approximation and in refs. [36,19,29,20]; whereas the QChPT result Eq. (37) has previously been calculated in ref. [12] for the mass-nondegenerate case with  $\alpha = \delta = 0$ , and in ref. [5] for the mass-nondegenerate case with  $\alpha = 0$ . We note a sign difference in the  $\delta$  term between Eq. (37) and the result in ref. [5].

Note that, apart from the usual nonanalytic cutoff dependence, nonanalytic functions depending on  $\epsilon$  appear in Eq. (37). This dependence is uniquely determined by (Q)ChPT, and predicts the dependence of  $B_K$  on  $m_\pi$  and  $m_K$  once the values of the low-energy constants  $K_i$ ,  $\tilde{K}$ ,  $F_i$  and  $\tilde{F}_j$  have been determined at a given value of the cutoff  $\Lambda$  from lattice results for  $B_K$  at given fixed values of these masses. Note that the contributions proportional to  $\delta$  and  $\alpha$  in  $B_K^q$  vanish in the mass-degenerate case,  $\epsilon = 0$ . (This is why we have not absorbed contact terms proportional to  $\alpha$  into  $\tilde{F}_1$  and  $\tilde{F}_3$ .) We see that, apart from a change from  $B^f$  to  $B^q$  and  $f$  to  $f_q$ , quenching does not introduce any change in the nonanalytic one-loop corrections of  $B_K$  in the mass-degenerate case. As we will see, such is not the case for the  $K^+ \rightarrow \pi^+\pi^0$  matrix element.

#### 4. $K^+ \rightarrow \pi^+\pi^0$ in the real world

The  $\Delta S = 1$ ,  $\Delta I = 3/2$   $K^+ \rightarrow \pi^+\pi^0$  decay amplitude is proportional to the weak matrix element

$$\langle \pi^+\pi^0 | (\bar{s}d\bar{u}u + \bar{s}u\bar{u}d - \bar{s}d\bar{d}d)_{LL} | K^+ \rangle . \quad (39)$$

The operator is the  $\Delta I = 3/2$  component of the same 27-plet that also contains the operator  $(\bar{s}d\bar{s}d)_{LL}$  (Eq. (23)). To lowest order in ChPT, the  $\Delta I = 3/2$   $O(p^2)$ -operator is represented by

$$O_4 = \alpha_{27} r_{kl}^{ij} (\Sigma \partial^\mu \Sigma^\dagger)_{ik} (\Sigma \partial_\mu \Sigma^\dagger)_{jl} , \quad (40)$$

where the tensor  $r_{kl}^{ij}$  has nonzero components

$$\begin{aligned} r_{31}^{21} = r_{13}^{12} = r_{31}^{12} = r_{13}^{21} &= \frac{1}{2} , \\ r_{32}^{22} = r_{23}^{22} &= -\frac{1}{2} \end{aligned} \quad (41)$$

(all other components vanish). It is easy to check that the tensor  $r_{kl}^{ij}$  satisfies condition Eq. (26) . The parameter  $\alpha_{27}$  is the same as in Eq. (25). This was used in ref. [21] to derive a tree-level relation between the  $K^+ \rightarrow \pi^+\pi^0$  decay rate and  $B_K$ : at tree level, using Eq. (29), we have

$$\langle \pi^+\pi^0 | O_4 | K^+ \rangle = \frac{12i\alpha_{27}}{\sqrt{2}f_\pi^3} (m_K^2 - m_\pi^2) = \frac{4i}{\sqrt{2}} f_\pi (m_K^2 - m_\pi^2) B_K . \quad (42)$$

Again, the factor  $m_K^2 - m_\pi^2$  arises from taking the kaon and pion momenta on shell, analogous to Eq. (28).

Bijnens *et al.* [16] were the first to investigate  $B_K$  and  $K^+ \rightarrow \pi^+\pi^0$  decay to one loop in ChPT. They used the approximation of vanishing pion mass based on the fact that, experimentally,  $m_\pi^2/m_K^2 \approx 1/13$ . Kambor *et al.* [18] gave a general analysis of strangeness-changing nonleptonic weak-decay processes involving up to four Goldstone mesons including  $K^+ \rightarrow \pi^+\pi^0$ , to one loop.

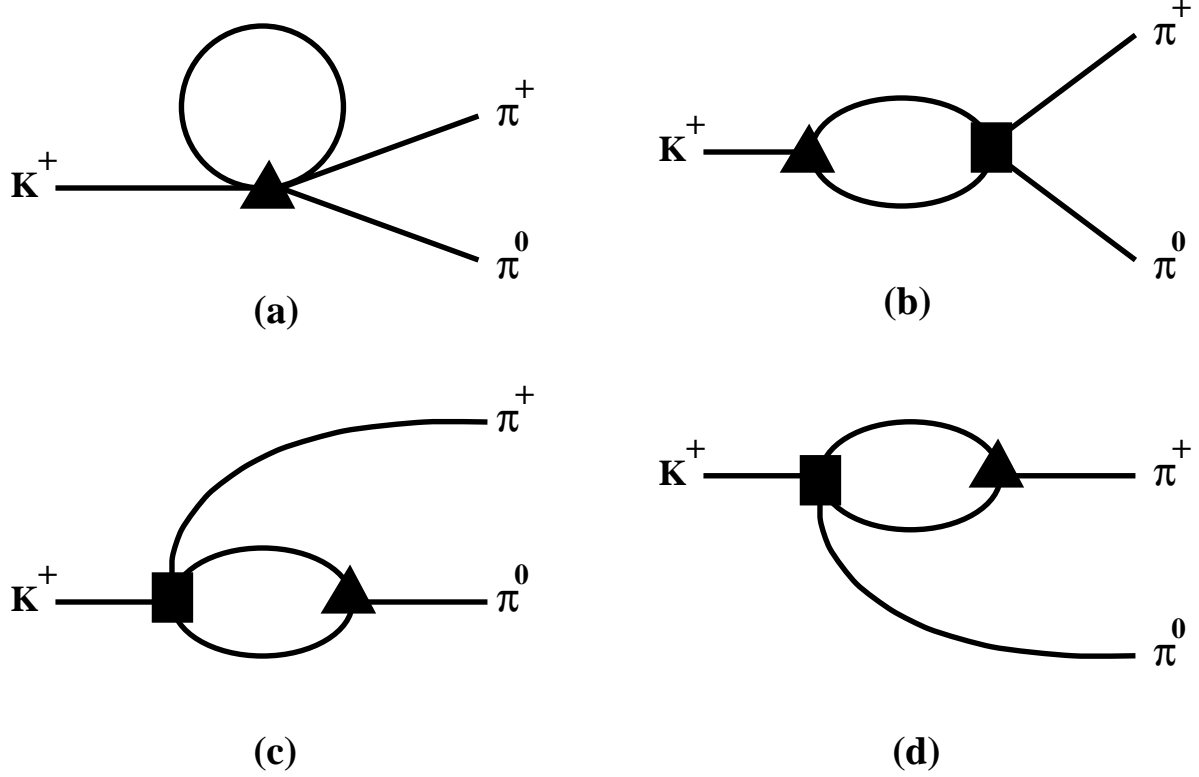


Figure 1. Feynman diagrams for the one-loop contributions to the  $K^+ \rightarrow \pi^+\pi^0$  matrix element of  $O_4$ . Filled triangles denote weak-interaction vertices and filled squares denote strong-interaction vertices.

We have repeated the calculation with nonzero pion mass and  $m_u = m_d \neq m_s$ . Loop corrections come from diagrams (a) to (d) in fig. 1 and, in addition, from wavefunction renormalizations. Our result is:

$$\begin{aligned}
\langle \pi^+\pi^0 | O_4 | K^+ \rangle = & \\
\frac{12i\alpha_{27}}{\sqrt{2}f_\pi^3} \left\{ (m_K^2 - m_\pi^2) \left[ 1 + \frac{m_K^2}{(4\pi f)^2} \left( I_z + I_f + \frac{13K_1}{6} - \frac{K_2}{3} - \left( \frac{K_1}{6} - \frac{7K_2}{3} \right) y_\pi + G_1 + G_2 y_\pi \right) \right] \right. & \\
& \left. + \frac{m_K^4}{(4\pi f)^2} (I_a + I_b + I_{c+d}) \right\}, & (43)
\end{aligned}$$

where

$$I_z = \frac{7}{6} \log \frac{m_K^2}{m_\pi^2} + \left[ \frac{1}{3} - \frac{1}{12} y_\pi \right] \log \frac{m_\eta^2}{m_\pi^2} + \frac{3}{2} [1 + y_\pi] \log \frac{m_\pi^2}{\Lambda^2},$$

$$\begin{aligned}
I_f &= -3 \log \frac{m_K^2}{m_\pi^2} - 3[1 + 2y_\pi] \log \frac{m_\pi^2}{\Lambda^2}, \\
I_a &= - \left[ \frac{13}{3} - 4y_\pi \right] \log \frac{m_K^2}{m_\pi^2} - \left[ \frac{4}{3} - y_\pi + \frac{1}{6}y_\pi^2 \right] \log \frac{m_\eta^2}{m_\pi^2} - \left[ \frac{17}{3} + y_\pi - \frac{20}{3}y_\pi^2 \right] \log \frac{m_\pi^2}{\Lambda^2}, \\
I_b &= \left[ 1 - 3y_\pi + 2y_\pi^2 \right] \left( A(y_\pi) + i \pi \sqrt{1 - 4y_\pi} \right) + \left[ 1 - \frac{13}{3}y_\pi + \frac{14}{3}y_\pi^2 \right] \log \frac{m_\pi^2}{\Lambda^2}, \\
I_{c+d} &= -\frac{4}{3y_\pi} + \frac{4}{3} - \left[ \frac{5}{8y_\pi^2} - \frac{13}{8y_\pi} + 1 \right] A(y_\pi) - \frac{1}{72} \left[ \frac{1}{y_\pi^2} - \frac{1}{y_\pi} \right] B(y_\pi) \\
&\quad + \left[ \frac{11}{18y_\pi^2} - \frac{23}{9y_\pi} + \frac{65}{18} - \frac{7}{3}y_\pi \right] \log \frac{m_K^2}{m_\pi^2} \\
&\quad + \left[ \frac{1}{72y_\pi^2} - \frac{23}{72y_\pi} + \frac{19}{18} - \frac{19}{12}y_\pi + \frac{1}{3}y_\pi^2 \right] \log \frac{m_\eta^2}{m_\pi^2} \\
&\quad + \frac{1}{3} \left[ 5 - 8y_\pi - y_\pi^2 \right] \log \frac{m_\pi^2}{\Lambda^2}. \tag{44}
\end{aligned}$$

The functions  $A(y_\pi)$  and  $B(y_\pi)$  are defined as follows:

$$A(y_\pi) = \sqrt{1 - 4y_\pi} \log \left( \frac{1 + \sqrt{1 - 4y_\pi}}{1 - \sqrt{1 - 4y_\pi}} \right), \tag{45}$$

$$B(y_\pi) = \sqrt{1 - 44y_\pi + 16y_\pi^2} \log \left( \frac{7 - 4y_\pi + \sqrt{1 - 44y_\pi + 16y_\pi^2}}{7 - 4y_\pi - \sqrt{1 - 44y_\pi + 16y_\pi^2}} \right). \tag{46}$$

The parameter  $y_\pi$  is defined in Eq. (13).  $I_z$  comes from wavefunction renormalizations (Eq. (8) and Eq. (10)), and  $I_f$  comes from converting  $f$  to  $f_\pi$  in the tree-level contribution to Eq. (43), using Eq. (7). The associated  $O(p^4)$  contact terms with coefficients  $K_i$  have been combined. (Note that refs. [18,19] keep the bare parameter  $f$  in the tree-level term.)  $I_a$  and  $I_b$  are nonanalytic one-loop corrections from diagrams (a) and (b) respectively, while we have combined those from diagrams (c) and (d) in  $I_{c+d}$ . The dimensionless parameters  $G_1$  and  $G_2$  come from  $O(p^4)$  weak operators [15]. We have again eliminated  $m_\eta^2$  in favor of  $m_\pi^2$  and  $m_K^2$  using Eq. (6) except in the  $\eta$  chiral logarithms. The imaginary term in  $I_b$  constitutes the lowest nontrivial order phase information for  $K^+ \rightarrow \pi^+ \pi^0$  decay from ChPT.

Analytic continuation of both  $A(y_\pi)$  and  $B(y_\pi)$  is understood for values of  $y_\pi$  for which the arguments of the square roots would be negative. Of particular interest to us is the function  $B(y_\pi)$ . The expression in Eq. (46) is applicable to the region extending from



$y_\pi = 0$  to the smaller of the two zeros of the argument of the square root, which is around 0.023. In the region between this value and the larger zero, which is around 2.7, the following expression should be used:

$$B(y_\pi) = -2\sqrt{-1 + 44y_\pi - 16y_\pi^2} \arctan\left(\frac{\sqrt{-1 + 44y_\pi - 16y_\pi^2}}{7 - 4y_\pi}\right). \quad (47)$$

The real-world value for  $y_\pi \approx 1/13$  falls into this second region as opposed to the point  $y_\pi = 0$  which belongs to the first region.

If we do the calculation with  $m_K = m_\pi$ , we find that the combined contribution of  $I_a$ ,  $I_b$  and  $I_{c+d}$  vanishes.

Setting  $m_\pi = 0$  in Eq. (43), we get:

$$\langle \pi^+ \pi^0 | O_4 | K^+ \rangle = \frac{12i\alpha_{27}m_K^2}{\sqrt{2}f_\pi^3} \left\{ 1 + \frac{m_K^2}{(4\pi f)^2} \left( -\frac{9}{2} \log \frac{m_K^2}{\Lambda^2} + i\pi + 3 \log \frac{4}{3} - \frac{7}{2} + \frac{13K_1}{6} - \frac{K_2}{3} + G_1 \right) \right\}. \quad (48)$$

The chiral logarithm of ref. [16] appears, in addition to nonzero constant terms. The numerical significance of this will be discussed in section 7.

## 5. $K^+ \rightarrow \pi^+ \pi^0$ matrix elements from the lattice

$K^+ \rightarrow \pi^+ \pi^0$  decay has been studied on the lattice by two groups [8,9,1,4], both of which used degenerate quark masses and the quenched approximation. On the lattice, a kaon  $K^+$  at rest is created at time  $t = 0$ , using an appropriate bilinear quark operator. At a much later time  $t_1$  a lattice version of the  $\Delta S = 1$  and  $\Delta I = 3/2$  weak operator in Eq. (39) annihilates the  $K^+$  and creates its decay products that include  $\pi^+$  and  $\pi^0$ . Finally, at a time  $t_2$  much later than  $t_1$ , by a judicious choice of annihilation operators, the two pions, both at rest (see below), are picked among the products and annihilated. While the equations in this section apply to both finite and infinite spatial volumes, we will focus on the torus which is

the case of interest to lattice computations. The whole process can be expressed in terms of the following correlation function:

$$C(t_2, t_1) \equiv \langle 0 | \pi^+(t_2) \pi^0(t_2) O_4(t_1) K^-(0) | 0 \rangle \quad (49)$$

$$= \sum_{n,m} \frac{1}{\langle n|n\rangle \langle m|m\rangle} \langle 0 | e^{Ht_2} \pi^+(0) \pi^0(0) e^{-Ht_2} | n \rangle \langle n | e^{Ht_1} O_4(0) e^{-Ht_1} | m \rangle \langle m | K^-(0) | 0 \rangle \quad (50)$$

$$\xrightarrow{t_2 \gg t_1 \gg 0} \frac{\langle 0 | \pi^+(0) \pi^0(0) | \pi^+ \pi^0 \rangle \langle \pi^+ \pi^0 | O_4(0) | K^+ \rangle \langle K^+ | K^-(0) | 0 \rangle}{\langle \pi^+ \pi^0 | \pi^+ \pi^0 \rangle \langle K^+ | K^+ \rangle} e^{-E_{2\pi}(t_2-t_1)} e^{-m_K t_1} , \quad (51)$$

where  $H$  is the QCD Hamiltonian,  $\pi^+(t_2) \equiv \int d^3\mathbf{x} \pi^+(\mathbf{x}, t_2)$  and similarly for  $\pi^0(t_2)$  and  $K^-(0)$ . These fields couple to mesons with zero momentum. The operator  $O_4(t_1) \equiv \int d^3\mathbf{x} O_4(\mathbf{x}, t_1)$  couples only to states with zero total momentum. The state  $|\pi^+ \pi^0\rangle$  is the zero-momentum two-pion state with lowest energy, and  $|K^+\rangle$  is a zero-momentum kaon state. The sums over  $n$  and  $m$  run over complete sets of states. Eq. (51) shows the leading term of Eq. (50) in the large-time limits. Note that  $E_{2\pi}$ , which denotes the energy of two pions at rest in a finite volume, deviates from its infinite-volume value  $2m_\pi$  [37,38].

We will also need the four-pion correlation function and the kaon propagator in order to extract the desired matrix element  $\langle \pi^+ \pi^0 | O_4(0) | K^+ \rangle$ :

$$\begin{aligned} \langle 0 | \pi^+(t_2) \pi^0(t_2) \pi^-(t_1) \pi^0(t_1) | 0 \rangle &= \sum_n \frac{1}{\langle n|n\rangle} \langle 0 | \pi^+(t_2) \pi^0(t_2) | n \rangle \langle n | \pi^-(t_1) \pi^0(t_1) | 0 \rangle \\ &\xrightarrow{t_2 \gg t_1} \frac{|\langle 0 | \pi^+(0) \pi^0(0) | \pi^+ \pi^0 \rangle|^2}{\langle \pi^+ \pi^0 | \pi^+ \pi^0 \rangle} e^{-E_{2\pi}(t_2-t_1)} , \end{aligned} \quad (52)$$

and

$$\begin{aligned} \langle 0 | K^+(t_1) K^-(0) | 0 \rangle &= \sum_n \frac{1}{\langle n|n\rangle} \langle 0 | K^+(t_1) | n \rangle \langle n | K^-(0) | 0 \rangle \\ &\xrightarrow{t_1 \gg 0} \frac{|\langle K^+ | K^-(0) | 0 \rangle|^2}{\langle K^+ | K^+ \rangle} e^{-m_K t_1} . \end{aligned} \quad (53)$$

Some comments are in order. First, after taking the square root of the factors in front of the exponentials in the large-time limits in Eq. (52) and Eq. (53), we can extract the desired

matrix element from Eq. (51) only if we know the normalizations of the state vectors. We choose the complete set of states to consist of single-particle eigenstates and their tensor products. We use the canonical relativistic normalization for single-particle states:

$$\langle K^+(\mathbf{p})|K^+(\mathbf{q})\rangle = 2L^3 E_K(\mathbf{p})\delta_{\mathbf{p},\mathbf{q}} , \quad (54)$$

where  $E_K(\mathbf{p})$  is the energy of the kaon with spatial momentum  $\mathbf{p}$ ,  $L^3$  is the spatial volume, and  $\delta_{\mathbf{p},\mathbf{q}}$  is the Kronecker delta, with similar definitions for other mesons. The normalizations for two-particle states are

$$\langle \pi^+(\mathbf{P})\pi^0(\mathbf{p})|\pi^+(\mathbf{Q})\pi^0(\mathbf{q})\rangle = \langle \pi^+(\mathbf{P})|\pi^+(\mathbf{Q})\rangle \langle \pi^0(\mathbf{p})|\pi^0(\mathbf{q})\rangle . \quad (55)$$

Second, the process corresponding to the large time leading order contribution in Eq. (51) does not conserve energy (except when  $m_K = 2m_\pi$ ). We will therefore refer to the matrix element  $\langle \pi^+\pi^0|O_4(0)|K^+\rangle$  as “unphysical.” The physical matrix element corresponds to an excited state in Eq. (50) if  $m_K > 2m_\pi$ , subleading in the large-time limits. In principle, since in this “unphysical” case  $O_4$  inserts momentum, its chiral representation could include total-derivative terms. However, there are no such terms to order  $p^2$ . It is clear that we are unable to uncover the phase of any matrix element, in accordance with the discussion in ref. [22].

## 6. Calculation of $\langle \pi^+\pi^0|O_4(0)|K^+\rangle$ in finite-volume (Q)ChPT

While lattice computations are done at a nonzero lattice spacing (an issue we will not address in this paper), they are also confined to a finite four-volume. We will take the finite spatial volume as a cube with linear dimension  $L$  on each side. Gasser and Leutwyler, among others [10], argued that when periodic boundary conditions are used, spatial finite-volume effects can be taken into account in ChPT by changing the (spatial) momentum integrals in

loop computations into discrete sums, *i.e.* for any function  $f(\mathbf{k})$ , the integral  $\int \frac{d^3\mathbf{k}}{(2\pi)^3} f(\mathbf{k})$  is changed into the sum  $\frac{1}{L^3} \sum_{\mathbf{k}} f(\mathbf{k})$ , where  $\mathbf{k} = 2\pi\mathbf{n}/L$  with  $\mathbf{n} \in \mathbb{Z}^3$ , the discrete momentum in the box. The prescription is valid up to corrections vanishing faster than any power of  $L^{-1}$ . On the other hand, the values of the coefficients of all  $O(p^2)$  and  $O(p^4)$  operators remain the same as in infinite volume, again up to corrections vanishing faster than any power of  $L^{-1}$ .

### A. Tree-level contribution

We will now describe the calculation of  $C(t_2, t_1)$  (Eq. (49)), in finite-volume ChPT. We will choose  $t_2 > t_1 > 0$ . We first show the relatively straightforward tree-level calculation in order to set up notation that will facilitate the discussion of the one-loop calculation. We define the  $\pi^+$  two-point function:

$$D_+(x, y) = \langle \pi^+(\mathbf{x}, t) \pi^-(\mathbf{y}, s) \rangle , \quad (56)$$

where  $x = (\mathbf{x}, t)$  and  $y = (\mathbf{y}, s)$  are space-time points. The two-point functions  $D_0$  and  $D_K$  for  $\pi^0$  and  $K^+$  are defined in a similar way. Defining the sign function

$$\text{sign}(t) = \begin{cases} 1, & t > 0 \\ 0, & t = 0 \\ -1, & t < 0 \end{cases} , \quad (57)$$

and

$$\xi_+^0 = 1 \quad , \quad \xi_+^r = -\xi_+^l = m_\pi \text{sign}(t - s) , \quad (58)$$

we have for the spatial integrals of the two-point function and its derivatives:

$$\begin{aligned} \int d^3\mathbf{x} D_+(x, y) &= \frac{\xi_+^0}{2m_\pi} e^{-m_\pi|t-s|} , \\ \int d^3\mathbf{x} \frac{\partial}{\partial y_\mu} D_+(x, y) &= \delta_{\mu 4} \frac{\xi_+^r}{2m_\pi} e^{-m_\pi|t-s|} , \\ \int d^3\mathbf{x} \frac{\partial}{\partial x_\mu} D_+(x, y) &= \delta_{\mu 4} \frac{\xi_+^l}{2m_\pi} e^{-m_\pi|t-s|} , \end{aligned} \quad (59)$$

with similar definitions of  $\xi_0$ 's and  $\xi_K$ 's associated with the two-point functions  $D_0$  and  $D_K$ , respectively.

At tree level, we substitute the relevant part of  $O_4(\mathbf{x}_1, t_1)$  contributing to the  $K^+$  decay:

$$O_4(\mathbf{x}_1, t_1) \rightarrow -\frac{4i\alpha_{27}}{\sqrt{2}f^3} \left( 4\pi^- \partial^\mu \pi^0 \partial_\mu K^+ - \partial^\mu \pi^- \pi^0 \partial_\mu K^+ - 3\partial^\mu \pi^- \partial_\mu \pi^0 K^+ \right) (\mathbf{x}_1, t_1), \quad (60)$$

where each field is taken at the same space-time point  $(\mathbf{x}_1, t_1)$ , into Eq. (49) and get

$$C(t_2, t_1) = -\frac{4i\alpha_{27}}{\sqrt{2}f^3} \int d^3\mathbf{x}_2 \int d^3\tilde{\mathbf{x}}_2 \int d^3\mathbf{x}_1 \int d^3\mathbf{x}_K \left( 4D_+(x_2, x_1) \partial^\mu D_0(\tilde{x}_2, x_1) \partial_\mu D_K(x_1, x_K) - \partial^\mu D_+(x_2, x_1) D_0(\tilde{x}_2, x_1) \partial_\mu D_K(x_1, x_K) - 3\partial^\mu D_+(x_2, x_1) \partial_\mu D_0(\tilde{x}_2, x_1) D_K(x_1, x_K) \right), \quad (61)$$

where  $x_1 = (\mathbf{x}_1, t_1)$ ,  $x_2 = (\mathbf{x}_2, t_2)$ ,  $\tilde{x}_2 = (\tilde{\mathbf{x}}_2, t_2)$ ,  $x_K = (\mathbf{x}_K, 0)$  and  $\partial_\mu = \frac{\partial}{\partial x_{1\mu}}$ . After integrating over spatial coordinates corresponding to the external particles, *i.e.*  $\mathbf{x}_2$ ,  $\tilde{\mathbf{x}}_2$  and  $\mathbf{x}_K$ , with the help of Eq. (58) and Eq. (59), an expression independent of  $\mathbf{x}_1$  is left.

Integrating over  $\mathbf{x}_1$  then gives a trivial volume factor  $L^3$ . The tree-level result is

$$C(t_2, t_1) = -\frac{4i\alpha_{27}L^3}{\sqrt{2}f^3} \frac{e^{-2m_\pi(t_2-t_1)}}{4m_\pi^2} \frac{e^{-m_K t_1}}{2m_K} \left( 4\xi_+^0 \xi_0^r \xi_K^l - \xi_+^r \xi_0^0 \xi_K^l - 3\xi_+^r \xi_0^r \xi_K^0 \right) \\ = \frac{12i\alpha_{27}L^3}{\sqrt{2}f^3} m_\pi (m_K + m_\pi) \frac{e^{-2m_\pi(t_2-t_1)}}{4m_\pi^2} \frac{e^{-m_K t_1}}{2m_K}. \quad (62)$$

Note that to this order  $E_{2\pi} = 2m_\pi$ . A comparison of mass prefactors in Eq. (62) and Eq. (42) already shows the difference between unphysical and physical matrix elements. We will extract the unphysical matrix element from  $C(t_2, t_1)$  after the discussion of one-loop corrections.

### B. One-loop contributions in full ChPT

In this subsection we discuss the one-loop contributions from diagrams (a) to (d) (see fig. 1). We will from now on restrict ourselves to the mass-degenerate case. Diagram (a) is the tadpole diagram generated by only the weak operator  $O_4(t_1)$ . All octet mesons appear on the loop. Diagrams (b) to (d) involve the  $O(p^2)$  strong-interaction four-point vertex ( $\mathcal{L}_{int}$ ). These contributions are of the form

$$C(t_2, t_1)(b, c, d) = -\langle \pi^+(t_2) \pi^0(t_2) \left( \int d^3\mathbf{x}_s dt_s \mathcal{L}_{int}(\mathbf{x}_s, t_s) \right) O_4(t_1) K^-(0) \rangle_c, \quad (63)$$

where  $\langle \dots \rangle_c$  denotes all connected Wick contractions, and where the relevant terms (cubic in the octet field  $\phi$  (Eq. (2)) of the weak operator  $O_4(t_1)$  are taken. They fall into different categories, represented by the different topologies of diagrams (b) to (d). Due to conservation of charge and isospin by the strong interaction vertex, only  $\pi^+$  and  $\pi^0$  appear on the loop in diagram (b). In diagrams (c) and (d), a kaon and a pion or eta appear on the loop. We first explain in detail the contribution represented by diagram (b). The two external pions are Wick-contracted with two pions out of the four pion fields in  $\mathcal{L}_{int}$ . The other pion fields in  $\mathcal{L}_{int}$  are Wick-contracted with two pions from  $O_4$ . The one field left in  $O_4$  is Wick-contracted with the external kaon. We will denote fields contracted between  $O_4$  and  $\mathcal{L}_{int}$  by a subscript “I.” For diagram (b), we end up with the product of

$$\left( \partial^\nu \pi_I^- \pi_I^0 \partial_\nu K^+ - \partial^\nu \pi_I^- \partial_\nu \pi_I^0 K^+ \right) (\mathbf{x}_1, t_1) \quad (64)$$

and

$$\left( -\pi^- \pi^0 \partial^\mu \pi_I^+ \partial_\mu \pi_I^0 - \partial^\mu \pi^- \partial_\mu \pi^0 \pi_I^+ \pi_I^0 + \frac{1}{2} \left[ \partial^\mu \pi^- \pi^0 + \pi^- \partial^\mu \pi^0 \right] \left[ \partial_\mu \pi_I^+ \pi_I^0 + \pi_I^+ \partial_\mu \pi_I^0 \right] + m_\pi^2 \pi^- \pi^0 \pi_I^+ \pi_I^0 \right) (\mathbf{x}_s, t_s), \quad (65)$$

from  $O_4$  and  $\mathcal{L}_{int}$  respectively, with a prefactor  $-8i\alpha_{27}/(\sqrt{2}f^5)$ . Fields without subscript  $I$  contract with external lines. This product leads to a proliferation of terms with different possible combinations of derivatives acting on the fields, so let us represent each term in Eq. (64) and Eq. (65) symbolically by

$$\sigma(\mathbf{x}_1, t_1) \sigma_I^2(\mathbf{x}_1, t_1) \quad \text{and} \quad \Phi^2(\mathbf{x}_s, t_s) \Phi_I^2(\mathbf{x}_s, t_s), \quad (66)$$

respectively. The fields  $\sigma$  and  $\Phi$  stand for pion or kaon fields and their derivatives. With Eq. (66), all terms in Eq. (63) corresponding to diagram (b) can be written as

$$\int d^3\mathbf{x}_2 \int d^3\tilde{\mathbf{x}}_2 \int d^3\mathbf{x}_1 \int d^3\mathbf{x}_K \int d^3\mathbf{x}_s \int dt_s \langle \pi^+(\mathbf{x}_2, t_2) \Phi(\mathbf{x}_s, t_s) \rangle \langle \pi^0(\tilde{\mathbf{x}}_2, t_2) \Phi(\mathbf{x}_s, t_s) \rangle \times \\ \langle \Phi_I(\mathbf{x}_s, t_s) \sigma_I(\mathbf{x}_1, t_1) \rangle \langle \Phi_I(\mathbf{x}_s, t_s) \sigma_I(\mathbf{x}_1, t_1) \rangle \times$$

$$\begin{aligned}
& \langle \sigma(\mathbf{x}_1, t_1) K^+(\mathbf{x}_K, 0) \rangle \\
&= \int dt_s \int d^3\mathbf{x}_s \int d^3\mathbf{x}_1 \frac{e^{-2m_\pi|t_2-t_s|}}{4m_\pi^2} \frac{e^{-m_K t_1}}{2m_K} \xi_+ \xi_0 \xi_K \times \\
& \quad \langle \Phi_I(\mathbf{x}_s, t_s) \sigma_I(\mathbf{x}_1, t_1) \rangle \langle \Phi_I(\mathbf{x}_s, t_s) \sigma_I(\mathbf{x}_1, t_1) \rangle . \quad (67)
\end{aligned}$$

The  $\xi$ -factors are chosen according to the prescription of Eq. (59), and possible associated factors  $\delta_{\mu 4}$  have not been displayed explicitly. At this point two simplifications occur. First, Lorentz contractions of derivatives on the same internal leg do not occur because of the fact that they come from the simple product of two Lorentz invariants  $O_4$  and  $\mathcal{L}_{int}$  (see Eq. (64) and Eq. (65)). Second, if a derivative is Lorentz-contracted with another one acting on a field contracted with an external field, only the 4-th component of the derivative survives, according to Eq. (59). Using the momentum representation of the pion two-point functions, we obtain:

$$\begin{aligned}
& \int dt_s \int d^3\mathbf{x}_s \int d^3\mathbf{x}_1 \frac{e^{-2m_\pi|t_2-t_s|}}{4m_\pi^2} \frac{e^{-m_K t_1}}{2m_K} \times \\
& \quad \int_k \int_l \mathcal{N} \frac{e^{-i(\mathbf{k} \cdot (\mathbf{x}_s - \mathbf{x}_1) + k_4(t_s - t_1))}}{(k^2 + m_\pi^2)} \frac{e^{-i(\mathbf{l} \cdot (\mathbf{x}_s - \mathbf{x}_1) + l_4(t_s - t_1))}}{(l^2 + m_\pi^2)} , \quad (68)
\end{aligned}$$

where

$$\mathcal{N} = -\frac{8i\alpha_{27}}{\sqrt{2}f^5} (-m_K \text{sign}(t_1) i k_4 + k^\mu l_\mu) (k^\mu l_\mu - m_\pi \text{sign}(t_2 - t_s) i(k_4 + l_4)) . \quad (69)$$

We use the abbreviation  $\int_k \equiv \frac{1}{L^3} \sum_{\mathbf{k}} \int \frac{dk_4}{2\pi}$  with  $\mathbf{k} = 2\pi\mathbf{n}/L$  and  $\mathbf{n} \in \mathbb{Z}^3$ . We then integrate over  $\mathbf{x}_1$ . This results in a delta function setting  $\mathbf{k} = -\mathbf{l}$ . Physically, this corresponds to the fact that  $O_4(t_1)$  only couples to states with zero total momentum. One of the momentum sums, say over  $\mathbf{l}$ , can be performed which leads to an integrand independent of  $\mathbf{x}_s$ , and subsequent integration over  $\mathbf{x}_s$  then gives a trivial volume factor  $L^3$ . The result is

$$L^3 \int dt_s \frac{e^{-2m_\pi|t_2-t_s|}}{4m_\pi^2} \frac{e^{-m_K t_1}}{2m_K} \frac{1}{L^3} \sum_{\mathbf{k}} \int \frac{dk_4}{2\pi} \int \frac{dl_4}{2\pi} \mathcal{N} \frac{e^{-ik_4(t_s-t_1)}}{(k_4^2 + \mathbf{k}^2 + m_\pi^2)} \frac{e^{-il_4(t_s-t_1)}}{(l_4^2 + \mathbf{k}^2 + m_\pi^2)} , \quad (70)$$

where  $\mathcal{N}$  now takes on the form:

$$\mathcal{N} = -\frac{8i\alpha_{27}}{\sqrt{2}f^5} \left( -m_K \text{sign}(t_1) i k_4 + k_4 l_4 - \mathbf{k}^2 \right) \left( k_4 l_4 - \mathbf{k}^2 - m_\pi \text{sign}(t_2 - t_s) i (k_4 + l_4) \right) .$$

The following formulas are needed for the evaluation of the integrals over  $k_4$  and  $l_4$  in Eq. (70):

$$\begin{aligned} & \int \frac{dk_4}{2\pi} \int \frac{dl_4}{2\pi} \mathcal{A} \frac{e^{-i(k_4+l_4)(t_s-t_1)}}{(k_4^2 + \omega_{\mathbf{k}}^2)(l_4^2 + \omega_{\mathbf{k}}^2)} \\ &= \begin{cases} \int \frac{dk_4}{2\pi} \delta(t_s - t_1) - \omega_{\mathbf{k}} \delta(t_s - t_1) + \frac{\omega_{\mathbf{k}}^2}{4} e^{-2\omega_{\mathbf{k}}|t_s-t_1|} , & \mathcal{A} = k_4^2 l_4^2 \\ \text{sign}(t_s - t_1) \left( \frac{1}{2} \delta(t_s - t_1) - \frac{\omega_{\mathbf{k}}}{4} e^{-2\omega_{\mathbf{k}}|t_s-t_1|} \right) , & \mathcal{A} = i k_4^2 l_4 \\ \frac{1}{2\omega_{\mathbf{k}}} \delta(t_s - t_1) - \frac{1}{4} e^{-2\omega_{\mathbf{k}}|t_s-t_1|} , & \mathcal{A} = k_4^2 \\ -\frac{1}{4} e^{-2\omega_{\mathbf{k}}|t_s-t_1|} , & \mathcal{A} = k_4 l_4 \\ \frac{1}{4\omega_{\mathbf{k}}} \text{sign}(t_s - t_1) e^{-2\omega_{\mathbf{k}}|t_s-t_1|} , & \mathcal{A} = i k_4 \\ \frac{1}{4\omega_{\mathbf{k}}^2} e^{-2\omega_{\mathbf{k}}|t_s-t_1|} , & \mathcal{A} = 1 \end{cases} \quad (71) \end{aligned}$$

where

$$\omega_{\mathbf{k}} = \sqrt{\mathbf{k}^2 + m_\pi^2} . \quad (72)$$

The strong interaction can “occur” at any time  $t_s$ , a fact reflected by the integration over  $t_s$  from  $-\infty$  to  $+\infty$ . Carrying out the integrating over  $t_s$  after integrating over  $k_4$  and  $l_4$ , we finally obtain for the contribution from diagram (b):

$$\begin{aligned} & \frac{24i\alpha_{27}L^3}{\sqrt{2}f^3} m_\pi^2 \frac{e^{-2m_\pi(t_2-t_1)}}{4m_\pi^2} \frac{e^{-m_K t_1}}{2m_K} \times \\ & \frac{1}{f^2 L^3} \left( -\frac{1}{2}(t_2 - t_1) + \frac{1}{24m_\pi} - \frac{1}{3m_\pi^2} \sum_{\mathbf{k}} \left[ \int \frac{dk_4}{2\pi} - \omega_{\mathbf{k}} - \frac{m_\pi^2}{2\omega_{\mathbf{k}}} \right] \right. \\ & \quad - \sum_{\mathbf{k} \neq 0} \frac{1}{\mathbf{k}^2} \left[ \frac{\omega_{\mathbf{k}}^3}{3m_\pi^2} + \frac{\omega_{\mathbf{k}}}{3} - \frac{m_\pi^2}{6\omega_{\mathbf{k}}} \right] \\ & \quad \left. + \sum_{\mathbf{k} \neq 0} \frac{1}{\mathbf{k}^2} \left[ \frac{2\omega_{\mathbf{k}}^2}{3m_\pi} + \frac{\omega_{\mathbf{k}}}{3} - \frac{m_\pi}{2} - \frac{m_\pi^2}{12\omega_{\mathbf{k}}} + \frac{m_\pi^3}{12\omega_{\mathbf{k}}^2} \right] e^{-2(\omega_{\mathbf{k}} - m_\pi)(t_2-t_1)} \right) . \quad (73) \end{aligned}$$

We distinguished  $m_K$  from  $m_\pi$  in the time exponentials even though we consider only the case  $m_K = m_\pi$ . Most momentum sums are divergent and have to be regularized. This will



be discussed in more detail when we get to the final expressions including also contributions from diagrams (a), (c) and (d). Here we only note that the term proportional to  $\int \frac{dk_4}{2\pi}$  cancels against similar terms from diagrams (c) and (d).

Of particular interest is the contribution from values of  $t_s$  between  $t_1$  and  $t_2$  and with  $\mathbf{k} = 0$ , which leads to the term proportional to  $t_2 - t_1$ . Physically, this corresponds to the subprocess in which the two pions created by  $O_4(t_1)$  are at rest and then scatter into the final pions, both also at rest, at any time between  $t_1$  and  $t_2$ . This term can be resummed into the time exponentials associated with the out-going pions of the tree-level contribution to  $C(t_2, t_1)$  in Eq. (62). (Since there are no such pion-rescattering sub-diagrams in diagrams (c) and (d) no similar resummation occurs in those cases.) This corresponds to the finite-volume correction to the energy of two pions at rest with isospin  $I = 2$ :

$$E_{2\pi} = 2m_\pi + \frac{1}{2L^3 f^2} . \quad (74)$$

This volume dependence agrees with the general analysis by Lüscher [38] of the finite-volume energy shifts of two-particle states. Here we only encounter the tree-level energy shift because the pion-pion scattering sub-diagram is a tree-level diagram.

The terms suppressed by a relative factor  $\exp[-2(\omega_{\mathbf{k}}^2 - m_\pi^2)(t_2 - t_1)]$  correspond to contributions from excited states. In fact, if  $m_K > 2m_\pi$  (a mass-nondegenerate situation), Eq. (50) indicates that the “physical” matrix element that conserves energy-momentum is among the nonleading terms. However, in a typical lattice computation,  $m_K < 2m_\pi$ , and the finite volume is exploited to obtain the leading term in the large-time limits ( $t_2 \gg t_1 \gg 0$ ) in which excited states are suppressed. Then, only the unphysical matrix element is obtained. We see that one-loop ChPT can be used in order to estimate the contamination from excited states, as well as the difference between the physical and unphysical matrix elements (see next section). See Appendix B for a discussion of the extraction of the  $I = 2$  pion scattering length from nonleading time exponentials for diagram (b) in infinite volume.

The calculation of diagrams (c) and (d) is very similar, and we will not discuss them here. In these cases, there are no pion-rescattering sub-diagrams.

### C. Calculation in QChPT

We now turn to the quenched calculation. As already mentioned in the second section, QChPT has an unphysical particle content. Therefore, there is no reason to believe that a well-defined Hamiltonian exists, and none of the manipulations of Eq. (50) are justified when applied to QChPT. The large-time behavior of Eq. (51) may not be realized. However, a Euclidean path-integral type calculation of  $C(t_2, t_1)$  to one loop in QChPT similar to the one in unquenched ChPT can be carried out. In particular, the tree-level contribution and the term proportional to  $t_2 - t_1$  that occurs in diagram (b) are identical to those in full ChPT. Resummation of the latter again gives the time exponentials for external legs as shown in Eq. (51) with  $E_{2\pi}$  as in Eq. (74). We will extract the matrix element  $\langle \pi^+ \pi^0 | O_4(0) | K^+ \rangle$  from the QChPT result for  $C(t_2, t_1)$  in the same way as in the unquenched case. Note that this prescription coincides with the method used in numerical work [8,9,1].

One of the differences between ChPT and QChPT is the explicit inclusion of the  $\eta'$  field in QChPT. The  $\eta'$  shows up in QChPT in two ways [11,25]: through arbitrary scalar functions of the  $\eta'$  field multiplying all terms in the Lagrangian and the weak operators, and as the ninth component of the nonet field, *cf.* Eq. (14). It is easy to check that in the case of interest, the scalar functions do not lead to new contributions. Furthermore, since the operator that represents the chiral currents is

$$\begin{aligned} (L_\mu^q)_{ij} &= \left( \Sigma_q \partial_\mu \Sigma_q^\dagger \right)_{ij} = \left( \left( e^{i\eta'/\sqrt{3}f_q} \Sigma \right) \partial_\mu \left( e^{-i\eta'/\sqrt{3}f_q} \Sigma^\dagger \right) \right)_{ij} \\ &= \left( -i \frac{\partial_\mu \eta'}{\sqrt{3}f_q} + \Sigma \partial_\mu \Sigma^\dagger \right)_{ij}, \end{aligned} \quad (75)$$

$\eta'$  couplings would in general arise from diagonal current elements. However, since

$$O_4 = \frac{1}{2} \alpha_{27}^q \left( L_{\mu 23}^q L_{11}^{q\mu} + L_{\mu 11}^q L_{23}^{q\mu} - L_{\mu 23}^q L_{22}^{q\mu} - L_{\mu 22}^q L_{23}^{q\mu} + L_{\mu 13}^q L_{21}^{q\mu} + L_{\mu 21}^q L_{13}^{q\mu} \right), \quad (76)$$

the  $\eta'$  decouples as a result of the cancellations that happen pairwise between the first and the third and the second and the fourth terms (for  $m_u = m_d$ ), and the particle content on the loops is the same as in ChPT. Since in the mass-degenerate case the double pole only occurs in  $\eta'$  two-point function, no contributions from the double pole show up here. As a result, the correlation function  $C(t_2, t_1)$  does not have  $\delta$  and  $\alpha$  dependence at one loop. Bad chiral behavior caused by double poles is absent.

#### D. Collected results from ChPT and QChPT

The one-loop corrected  $C(t_2, t_1)$  consists of the tree-level term and the one-loop contributions of diagrams (a) to (d) (for wavefunction renormalizations, see below). Dropping contributions from excited states, we obtain for the full and quenched theories, in that order:

$$C^f(t_2, t_1) = \frac{24i\alpha_{27}m_\pi^2L^3}{\sqrt{2}f^3} \frac{e^{-E_{2\pi}(t_2-t_1)-m_K t_1}}{8m_\pi^2 m_K} \times \left( 1 + \frac{m_\pi^2}{3f^2} \left[ \frac{1}{8(m_\pi L)^3} + C(m_\pi L) + D(m_\pi L) \right] + \frac{m_\pi^2}{(4\pi f)^2} P \right) \quad (77)$$

and

$$C^q(t_2, t_1) = \frac{24i\alpha_{27}^q m_\pi^2 L^3}{\sqrt{2}f_q^3} \frac{e^{-E_{2\pi}(t_2-t_1)-m_K t_1}}{8m_\pi^2 m_K} \times \left( 1 + \frac{m_\pi^2}{3f_q^2} \left[ \frac{1}{8(m_\pi L)^3} + C(m_\pi L) + \tilde{D}(m_\pi L) \right] + \frac{m_\pi^2}{(4\pi f_q)^2} \tilde{P} \right), \quad (78)$$

where

$$\begin{aligned} C(m_\pi L) &= -\frac{1}{(m_\pi L)^3} \sum_{\mathbf{k} \neq 0} \frac{1}{\mathbf{k}^2} \left( \frac{\omega_{\mathbf{k}}^3}{m_\pi} + m_\pi \omega_{\mathbf{k}} - \frac{m_\pi^3}{2\omega_{\mathbf{k}}} \right), \\ D(m_\pi L) &= +\frac{1}{(m_\pi L)^3} \sum_{\mathbf{k}} \left( \frac{\omega_{\mathbf{k}}}{m_\pi} - 13 \frac{m_\pi}{\omega_{\mathbf{k}}} + \frac{3}{4} \frac{m_\pi^3}{\omega_{\mathbf{k}}^3} \right), \\ \tilde{D}(m_\pi L) &= +\frac{1}{(m_\pi L)^3} \sum_{\mathbf{k}} \left( \frac{\omega_{\mathbf{k}}}{m_\pi} - 4 \frac{m_\pi}{\omega_{\mathbf{k}}} + \frac{3}{4} \frac{m_\pi^3}{\omega_{\mathbf{k}}^3} \right), \end{aligned} \quad (79)$$

and  $\omega_{\mathbf{k}}$  is defined in Eq. (72). The contact-term coefficients  $P$  and  $\tilde{P}$  come from  $O(p^4)$  weak operators for the full and quenched theories, respectively. Since this result does not

correspond to the physical weak matrix element, there is no simple relation between  $P$  and  $G_1$  and  $G_2$  in Eq. (43). Again, we distinguish between  $m_\pi$  and  $m_K$  in the prefactor for illustrative purpose only. The term proportional to  $t_2 - t_1$  in Eq. (73) has been resummed using Eq. (74).

In order to extract the unphysical matrix element from  $C(t_2, t_1)$ , we need the four-pion correlation function Eq. (52) to lowest nontrivial order in ChPT (with  $f \rightarrow f_q$  in the quenched case):

$$\langle 0 | \pi^+(t_2) \pi^0(t_2) \pi^-(t_1) \pi^0(t_1) | 0 \rangle = \frac{e^{-E_{2\pi}(t_2-t_1)}}{4m_\pi^2} L^6 \left( 1 + \frac{m_\pi^2}{12f^2} \frac{1}{(m_\pi L)^3} \right). \quad (80)$$

The second term in parentheses is the lowest nontrivial order finite-volume correction for the two-pion wavefunction-renormalization. (Note that such terms also occur in Eq. (77) and Eq. (78)). We also need the free kaon propagator (Eq. (53)):

$$\langle 0 | K^+(t_1) K^-(0) | 0 \rangle = \frac{L^3}{2m_K} e^{-m_K t_1}. \quad (81)$$

A cutoff is assumed to regulate the divergent momentum sums in the functions  $C$ ,  $D$  and  $\tilde{D}$  defined in Eq. (79). The quartic divergences present in the individual terms cancel in the combinations  $C + D$  and  $C + \tilde{D}$  in Eq. (77) and Eq. (78), respectively. The quadratic divergence is independent of  $m_\pi$  and can be absorbed into  $\alpha_{27}$  or  $\alpha_{27}^q$ . Note that the quadratic divergences for the full and quenched theories are not the same. This is another indication that the coefficients  $\alpha_{27}$  and  $\alpha_{27}^q$  of the ChPT and QChPT weak operators are different. The remaining logarithmic cutoff dependence can be absorbed into the coefficients  $P$  and  $\tilde{P}$ .

For large  $L$ , we can estimate the size of  $m_\pi$  dependence of the functions  $D$  and  $\tilde{D}$  by replacing the sum  $\frac{1}{L^3} \sum_{\mathbf{k}}$  by an integral  $\int \frac{d^3\mathbf{k}}{(2\pi)^3}$ , with corrections vanishing faster than any power of  $L^{-1}$ . The summand in the function  $C$  is singular for  $\mathbf{k} = 0$ , and powers of  $L^{-1}$  appear when we convert the sum to an integral. See Appendix C for details. In a finite volume, similar momentum sums also appear in the one-loop results for the weak

decay constants and wavefunction renormalizations quoted in section 2. These sums are not singular near  $\mathbf{k} = 0$ , and we can replace the sums with integrals as for the functions  $D$  and  $\tilde{D}$  above, with corrections vanishing faster than any power of  $L^{-1}$ . This leads to the expressions given in section 2.

When the appropriate division is carried out in order to extract the unphysical weak matrix element, the finite-volume two-pion wavefunction-renormalization corrections (terms  $\propto 1/L^3$ ) in Eq. (77) or Eq. (78) and Eq. (80) cancel. The matrix element thus obtained is renormalized by multiplying it by the wavefunction-renormalization factor  $Z_\pi\sqrt{Z_K}$  (Eq. (8) and Eq. (10) for the full theory and Eq. (19) and Eq. (21) for the quenched theory). We also make use of state normalizations Eq. (54) and Eq. (55). The mass-degenerate ( $m_u = m_d = m_s$ ) one-loop corrected renormalized unphysical weak matrix elements for the full and quenched theories in a finite volume  $L^3$  then are, respectively:

$$\langle \pi^+ \pi^0 | O_4(0) | K^+ \rangle^f = \frac{24i\alpha_{27} m_\pi^2 L^3}{\sqrt{2} f^3} \left( 1 + \frac{m_\pi^2}{(4\pi f)^2} \left[ -6 \log \frac{m_\pi^2}{\Lambda^2} + F(m_\pi L) + P - K_1 - K_2 \right] \right) \quad (82)$$

and

$$\langle \pi^+ \pi^0 | O_4(0) | K^+ \rangle^q = \frac{24i\alpha_{27}^q m_\pi^2 L^3}{\sqrt{2} f_q^3} \left( 1 + \frac{m_\pi^2}{(4\pi f_q)^2} \left[ -3 \log \frac{m_\pi^2}{\Lambda^2} + F(m_\pi L) + \tilde{P} - \tilde{K} \right] \right), \quad (83)$$

up to corrections vanishing faster than any power of  $L^{-1}$ , where the function

$$F(m_\pi L) = \frac{17.827}{m_\pi L} + \frac{12\pi^2}{(m_\pi L)^3} \quad (84)$$

is the finite-volume correction calculated in Appendix C. Note that the same finite-volume correction occurs in both full and quenched theories. (This is because diagram (b) is the same in the full and quenched theories, and because only diagram (b) gives rise to finite-volume corrections.)  $m_\pi$  is the measured meson mass. Contact terms with coefficients  $K_{1,2}$  and  $\tilde{K}$

come from wavefunction renormalizations. By comparing Eq. (82) and Eq. (83), aside from a change from  $\alpha_{27}$  to  $\alpha_{27}^q$  and  $f$  to  $f_q$ , we see a substantial change to the nonanalytic one-loop corrections due to quenching. If we would trade the parameter  $f$  for  $f_\pi$  in the tree-level term of the full theory result, the numerical factor multiplying the chiral logarithm would be  $-15$  instead of  $-6$  in Eq. (82), while there would be no change for the quenched result since  $f_q = f_\pi$  up to  $O(p^4)$  contact terms in that case. Because of translation invariance, the matrix elements of  $O_4(\mathbf{x}_1, 0)$  are trivially obtained by omitting the factor  $L^3$  from Eq. (82) and Eq. (83).

We end this section with a few remarks about one-loop contributions in the mass non-degenerate case ( $m_u = m_d \neq m_s$ ). Due to the mixing of  $\eta'$  and  $\eta$ , the  $\eta$  two-point function acquires a double pole and hence  $\alpha$  and  $\delta$  dependence ( $m_u = m_d$  prevents mixing of  $\pi^0$  with  $\eta$  and  $\eta'$ ). The  $\eta$  that appears on the loop of tadpole diagram (a) contributes in a way analogous to the way  $\eta$ -tadpoles contribute to quenched  $f_K$ . Hence, we expect the  $\delta$ -dependent term to be singular in the chiral limit, like in Eq. (20). The contribution from diagram (b) remains the same as in the mass-degenerate case, because only pions appear on the loop. We therefore expect that no “enhanced finite-volume corrections” such as in the case of pion scattering [30] at one loop. As for diagrams (c) and (d), virtual mesons of different masses appear on the loop. In particular,  $\eta$  appears and gives rise to double poles, and hence  $\alpha$  and  $\delta$  dependence, but no enhanced finite-volume corrections.

## 7. Numerical examples and discussion

Little or nothing is known about the values of the low-energy constants  $F_i$ ,  $\tilde{F}_j$ ,  $G_i$ ,  $P$  and  $\tilde{P}$  in Eqs. (30,32,43,82,83). (For some phenomenological information on the  $F$ 's and  $G$ 's, see refs. [18,19]; for the others no information is available at all.) Because of this situation, we will choose reasonable values of the cutoff  $\Lambda$  and ignore the contact terms in an attempt

to estimate the size of one-loop corrections. Values of the cutoff we will use in the following are 770 MeV (the mass of the  $\rho$ ) and 1 GeV. We note that in refs. [25,18,19] the value of the  $\eta$  mass was used as cutoff in a phenomenological analysis of  $O(p^4)$  contact terms. This makes the loop diagrams artificially small, which therefore would most likely underestimate the size of the  $O(p^4)$  corrections when we set the contact terms equal to zero.

The determination of the relative size of tree-level and one-loop contributions to the kaon matrix elements is particularly sensitive to the definition of the low-energy parameter  $\alpha_{27}$ , especially in any scheme that has nonvanishing quadratic divergences. Such divergences are subtracted by renormalizing  $\alpha_{27}$ , and this introduces an arbitrariness into the determination of the relative size of tree-level and one-loop contributions. We will ignore this ambiguity in some of what follows, and we will consider a quantity which is independent of  $\alpha_{27}$  at the end of this section.

Apart from the fact that the  $\eta'$  is light in QChPT, the same considerations concerning the choice of the cutoff values that apply in ChPT are also applicable in QChPT. Note that the cutoff in the quenched theory does not have to be same as that in the full theory. However, since non-Goldstone hadron masses in quenched QCD are roughly the same as in full QCD, we will again take the cutoff  $\Lambda_q$  for QChPT to be 770 MeV or 1 GeV. In the following numerical examples, we have used  $f_\pi = 132$  MeV,  $m_\pi = 136$  MeV,  $m_K = 496$  MeV, unless otherwise stated.  $m_\eta$  has been determined from Eq. (6).

#### A. $K^+ \rightarrow \pi^+\pi^0$ decay in the real world

For  $m_\pi = 0$ , from Eq. (48), ignoring  $O(p^4)$  contact terms, at  $\Lambda = 1$  GeV and  $\Lambda = 770$  MeV we find  $0.33 + 0.28i$  and  $0.12 + 0.28i$  respectively for the relative size of the one-loop correction to the tree-level term of the  $K^+ \rightarrow \pi^+\pi^0$  matrix element at  $m_\pi = 0$ . This is smaller than what one would obtain from the results of ref. [16], which (for the real parts) would give 0.57 and 0.35, respectively. This is due to the fact that in Eq. (48) we

kept contributions from the nonanalytic terms that become numerical constants after setting  $m_\pi = 0$ . This example demonstrates that estimates of the relative size of one-loop corrections are quite sensitive to the choice of the values of  $O(p^4)$  low-energy constants, or, equivalently, the cutoff, for quantities involving kaons. In addition, this matrix element is quite sensitive to the value of the pion mass, as one finds by substituting  $m_\pi = 136$  MeV in Eq. (43) with  $O(p^4)$  contact terms ignored, which gives considerably larger relative one-loop contributions for the real parts:  $0.63 + 0.20i$  and  $0.36 + 0.20i$  respectively. ( $B_K$ , in Eq. (36), is much less sensitive to the value of  $m_\pi$ .)

It is instructive to estimate the change in magnitude of  $O(p^4)$  contact terms due to a change in cutoff. This change can be calculated from Eq. (43), given two values of the cutoff. For the  $m_\pi = 0$  case, a change of  $\Lambda$  from 1 GeV to 770 MeV induces a change  $\Delta\widehat{G}_1 = 2.35$ . For the  $m_\pi = 136$  MeV case, one finds  $\Delta(\widehat{G}_1 + y_\pi\widehat{G}_2) = 2.96$ . Here, we defined  $\widehat{G}_1 = G_1 + \frac{13}{6}K_1 - \frac{1}{6}K_2$  and  $\widehat{G}_2 = G_2 - \frac{1}{6}K_1 + \frac{7}{3}K_2$ . Since the changes in  $\widehat{G}_{1,2}$  are of order one, we believe that using values for the cutoff of 770 MeV and 1 GeV gives a reasonable estimate of the uncertainty in the size of one-loop corrections coming from our ignorance of the values of the  $O(p^4)$  low-energy constants [39].

### B. $K^+ \rightarrow \pi^+\pi^0$ decay on the lattice

The physical and unphysical  $K^+ \rightarrow \pi^+\pi^0$  matrix elements in the full theory can be related up to one loop using Eq. (43) and Eq. (82):

$$\langle \pi^+\pi^0 | O_4(0) | K^+ \rangle_{phys} = X \frac{m_K^2 - m_\pi^2}{2M_\pi^2} \langle \pi^+\pi^0 | O_4(0) | K^+ \rangle_{unphys}^f, \quad (85)$$

where

$$X = \frac{1 + U + \frac{m_K^2}{(4\pi f_\pi)^2} \left[ -\frac{5K_1}{6} - \frac{K_2}{6} + G_1 - \left( \frac{K_1}{6} + \frac{2K_2}{3} - G_2 \right) y_\pi \right]}{1 + \frac{M_\pi^2}{(4\pi F_\pi)^2} \left[ -6 \log \frac{M_\pi^2}{\Lambda^2} + F(M_\pi L) + P - K_1 - K_2 \right]}, \quad (86)$$

where the subscript “(un)phys” refers to the (un)physical matrix element (we imagine the unphysical matrix element to be obtained from a lattice computation), and the superscript



“ $f$ ” refers to the full theory. Eq. (85) relates the real-world matrix element to the mass-degenerate unphysical matrix element as it would be computed on the lattice with degenerate quark masses. The relation is obtained by reconverting the factor  $1/f_\pi^3$  back to  $1/f^3$  in Eq. (43). The one-loop corrections in the resulting expression after this change are those given in Eq. (43), but without  $I_f$ , and now the  $O(p^4)$  contact terms are as in the numerator of Eq. (86). The parameter  $U$ , then, is the ratio of the nonanalytic one-loop contribution and the tree-level contribution in Eq. (43), leaving out  $I_f$ :

$$U = \frac{m_K^2}{(4\pi f_\pi)^2} \left( I_z + \frac{m_K^2}{m_K^2 - m_\pi^2} (I_a + I_b + I_{c+d}) \right), \quad (87)$$

and equals 0.089 or  $-0.015$  for  $\Lambda = 1$  GeV or  $\Lambda = 770$  MeV respectively (we will ignore the imaginary part of  $U$ , since it does not contribute to the magnitude of the amplitude to order  $p^4$ ). We use upper-case symbols  $F_\pi$  and  $M_\pi$  for the decay constant and meson mass as they would be computed on the lattice, and lower-case symbols for the real-world values of these quantities. At tree level,  $X = 1$ . Note that the ratio  $X$  is independent of  $\alpha_{27}$ , so that it is not sensitive to ambiguities in the renormalization of this parameter. Note also that the  $O(p^4)$  contact terms do not cancel between the numerator and denominator of Eq. (86).

If we take values for the pion mass and the volume typical for lattice computations, for example  $M_\pi = 0.4$  GeV,  $M_\pi L = 8$ , and  $F_\pi = f_\pi$  (and again set the  $O(p^4)$  low-energy constants equal to zero), we find the denominator of  $X$  to be about 1.8 (leading to  $X \approx 0.6$ ) for  $\Lambda = 1$  GeV, and about 1.6 (again leading to  $X \approx 0.6$ ) for  $\Lambda = 770$  MeV.

Actual lattice computations have all been done in the quenched approximation [8,9,1], and it is therefore interesting to compare the full physical and quenched unphysical (mass-degenerate) matrix elements directly. In this case, we find, using Eq. (43) and Eq. (83)

$$\langle \pi^+ \pi^0 | O_4(0) | K^+ \rangle_{phys} = Y \frac{\alpha_{27}}{\alpha_{27}^q} \left( \frac{f_q}{f} \right)^3 \frac{m_K^2 - m_\pi^2}{2M_\pi^2} \langle \pi^+ \pi^0 | O_4(0) | K^+ \rangle_{unphys}^q, \quad (88)$$

with

$$Y = \frac{1 + U + \frac{m_K^2}{(4\pi f_\pi)^2} \left[ -\frac{5K_1}{6} - \frac{K_2}{6} + G_1 - \left( \frac{K_1}{6} + \frac{2K_2}{3} - G_2 \right) y_\pi \right]}{1 + \frac{M_\pi^2}{(4\pi F_\pi)^2} \left[ -3 \log \frac{M_\pi^2}{\Lambda_q^2} + F(M_\pi L) + \tilde{P} - \tilde{K} \right]}, \quad (89)$$

where  $\Lambda_q$  is the cutoff in QChPT. Again, at tree level  $Y = 1$ . In this case there is no reason that  $\alpha_{27} = \alpha_{27}^q$  (or  $f = f_q$ ), since we are not comparing matrix elements in the same theory. In particular, Eq. (88) is sensitive to renormalization ambiguities in these parameters.

Lattice parameters	$M_\pi^2$	$M_\pi L$	$Y_{(1)}^{(1)}$	$Y_{(0.77)}^{(0.77)}$	$Y_{(0.77)}^{(1)}$	$Y_{(1)}^{(0.77)}$
$16^3 \times 25$ (or $\times 33$ )	0.168	6.55	0.72	0.69	0.77	0.65
$\beta = 5.7$ or	0.263	8.20	0.68	0.67	0.75	0.61
$1/a = 1.0$ GeV	0.474	11.0	0.65	0.70	0.77	0.59
$24^3 \times 40$	0.303	7.77	0.65	0.66	0.72	0.59
$\beta = 6$ or	0.428	9.24	0.63	0.67	0.74	0.57
$1/a = 1.7$ GeV						

Table 1. The factor  $Y$ , Eq. (89), with contact terms ignored, at different values of  $M_\pi^2$  for different combinations of values of the cutoff  $\Lambda$  and  $\Lambda_q$  for the full and quenched theories respectively. Lattice parameters including the four-volume  $L^3 \times T$  are shown. The superscript on  $Y$  denotes  $\Lambda$  in GeV; the subscript on  $Y$  denotes  $\Lambda_q$  in GeV.  $M_\pi^2$  is in  $\text{GeV}^2$ .

The tree-level relation ( $Y = 1$ ) was used in refs. [9,1,4] in order to extract the physical weak matrix element from the unphysical one computed on the lattice, assuming  $\alpha_{27} = \alpha_{27}^q$  and  $f = f_q$ . It was found that the lattice values, corrected in this way, were at least 50% larger than the experimental value. It is therefore interesting to estimate the values of the one-loop correction factor  $Y$ . We will again set the  $O(p^4)$  low-energy constants equal to zero, and consider two values of the cutoff, 1 GeV and 770 MeV, for both the full and quenched cases. Since these are different theories, there is no reason that the cutoff should be chosen the same in the numerator and denominator of Eq. (89), and we will compute four different values of  $Y$  for each  $M_\pi$  corresponding to the four possible different choices of the cutoffs in both theories. We will take the spread in the values of  $Y$  obtained in this way as an estimate

of the uncertainty in  $Y$ . Using  $F_\pi = f_\pi$ , and values for  $M_\pi$  and  $L$  from refs. [4,1], we report the values of  $Y$  summarized in table 1.

In order to get an idea about the size of finite-volume effects on  $Y$ , we list in table 2 the values of  $Y$  without the finite-volume correction  $F(M_\pi L)$  in Eq. (89).

Lattice parameters	$M_\pi^2$	$Y_{(1)}^{(1)}$	$Y_{(0.77)}^{(0.77)}$	$Y_{(0.77)}^{(1)}$	$Y_{(1)}^{(0.77)}$
$16^3 \times 25$ (or $\times 33$ )	0.168	0.82	0.80	0.88	0.74
$\beta = 5.7$ or	0.263	0.79	0.80	0.88	0.71
$1/a = 1.0$ GeV	0.474	0.79	0.88	0.98	0.71
$24^3 \times 40$	0.303	0.78	0.81	0.89	0.71
$\beta = 6$ or	0.428	0.78	0.86	0.95	0.71
$1/a = 1.7$ GeV					

Table 2. The factor  $Y$ , Eq. (89), with both contact terms and finite-volume correction  $F(M_\pi L)$  ignored. For further explanation, see the caption of table 1.

It is evident from a comparison of tables 1 and 2 that the finite-volume correction can be substantial, of order 10–20 %. Note that the finite-volume corrections do not take into account any corrections vanishing faster than any power of  $L^{-1}$ . While these are very small at large values of  $M_\pi L$ , they may be substantial for the values considered here [30]. We do not address this issue further in this paper. Of course, it should be stressed that these estimates of the correction factor  $Y$  do not take into account the factors  $\alpha_{27}/\alpha_{27}^q$  and  $(f_q/f)^3$  in Eq. (88). The fact that quadratic divergences differ between the full and quenched theories (*cf.* section 6.D) may be a hint that the ratio  $\alpha_{27}/\alpha_{27}^q$  is not very close to one.

The values of  $Y$  in tables 1 and 2 were evaluated by first calculating the numerator and denominator of Eq. (89), and then dividing the results. We could also have first calculated the  $O(p^4)$  terms in the numerator and denominator, and then evaluated  $Y$  as one plus the difference of these  $O(p^4)$  terms, since, in order to distinguish between these two methods, a two-loop calculation would be necessary. Since the values for  $Y$  in tables 1 and 2 differ

from one by rather substantial amounts, we would obtain significantly different results for  $Y$ . In fact, the average values of  $Y$  would have been lowered by about 10–20 % (relative to one). This difference reflects the uncertainty introduced by cutting off the chiral expansion at one-loop order.

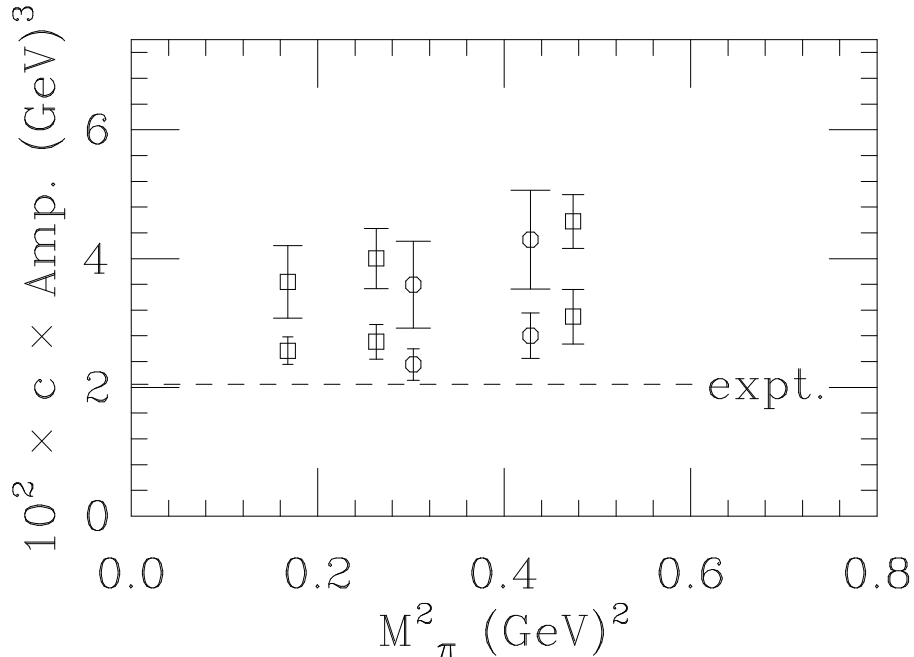


Figure 2. The physical  $K^+ \rightarrow \pi^+\pi^0$  amplitude vs.  $M_\pi^2$  from tree-level and one-loop (Q)ChPT. The one-loop corrected points lie below the tree-level corrected points. For detailed explanation, see text. Squares and octagons refer to data with four-volume  $16^3 \times 25$  (or  $\times 33$ ) and  $\beta = 5.7$  and four-volume  $24^3 \times 40$  and  $\beta = 6$  in table 1, respectively.  $c = 2\sqrt{2}/(G_F \sin\theta_c \cos\theta_c)$ .

In fig. 2, we replot some of the lattice data in fig. 16 of ref. [4] (or fig. 3 of ref. [1]) for the  $K^+ \rightarrow \pi^+\pi^0$  matrix element at different values of  $M_\pi^2$  (errors are statistical). We chose data with  $M_\pi < 770$  MeV and with the larger spatial volume for  $\beta = 6$ . The  $M_\pi$  and  $L$  values are those used in tables 1 and 2. These points have already been corrected for the difference between physical and unphysical values using tree-level ChPT, assuming

$\alpha_{27} = \alpha_{27}^q$  and  $f = f_q$ . Again assuming these equalities, we also plot the one-loop corrected physical matrix element using Eq. (88) with values of  $Y$  as shown in table 1. In all cases, the one-loop corrected points lie below the tree-level corrected points. At each point, the central value is obtained using the average of the four different values of  $Y$ , while the error bar is obtained from the largest and smallest values of  $Y$ . These error bars do not include the statistical errors of the lattice computation. We see that the one-loop corrected values are closer to the experimental value.

We end this sub-section with some discussion of the  $O(p^4)$  low-energy constants and the contributions from excited states to the correlation function Eq. (49).

First, we note that, for the quenched unphysical weak matrix element Eq. (83), a change of cutoff  $\Lambda_q$  from 1 GeV to 770 MeV results in a shift  $\Delta(\tilde{P} - \tilde{K}) = 1.57$ , again of order one.

Due to the fact that quenched and full QCD are different theories, there is no relation between the low-energy constants  $\tilde{P}$ ,  $\tilde{K}$  and  $G_{1,2}$ ,  $K_{1,2}$ , and therefore, in principle, no cancellation occurs in Eq. (89). Alternatively, at small enough  $M_\pi$ , one may envision relating physical and unphysical weak matrix elements, both in the full theory, as in Eq. (85) when realistic lattice computations for full QCD become possible. However, since the unphysical matrix element is calculated at different external four-momenta, the contact terms  $P$  for the unphysical full matrix element, Eq. (82), and  $G_{1,2}$  again have no simple relation, and again no cancellation takes place in Eq. (86). While in principle the constants  $\tilde{P}$ ,  $\tilde{K}$ ,  $P$ ,  $K_1$  and  $K_2$  can be obtained from the lattice, this is not the case for  $G_1$  and  $G_2$  as long as only matrix elements with all mesons at rest are computed numerically. The values of coefficients  $K_1$  and  $K_2$  associated with weak decay constants have been constrained in ref. [25] (where a different notation is used) with the help of large- $N_c$  arguments. A larger number of  $O(p^4)$  operators contribute to  $K^+$  decay, and in Eq. (43),  $G_1$  and  $G_2$  are actually particular linear combinations of the associated coefficients. A determination of some of the coefficients in the  $m_\pi = 0$  approximation has been attempted in refs. [18,19].

A determination of the prefactor  $(f_q/f)^3$  requires a more precise knowledge of weak decay constants both in full and quenched theories in the chiral limit than appears to be available at the moment. A fit of quenched lattice data for  $F_\pi$  in the mass-degenerate case to Eq. (18) would give  $f_q$  and  $\tilde{K}$  [40], but  $f$ ,  $K_1$  and  $K_2$  are only poorly known from phenomenology [25]. In addition, nothing is known about the ratio  $\alpha_{27}/\alpha_{27}^q$ . As long as no more detailed knowledge of all low-energy constants involved is available, we are limited to the estimates of ChPT one-loop effects as presented in this paper.

In order to separate the contribution of the lowest two-pion state (for which each pion has spatial momentum  $\mathbf{k} = 0$ ) from that of the closest excited states (for which each pion has spatial momentum  $|\mathbf{k}| = 2\pi/L$  (*cf.* Eq. (73))) to Eq. (49), we demand that

$$\Omega = 2M_\pi t \left( \sqrt{1 + \left( \frac{2\pi}{M_\pi L} \right)^2} - 1 \right) \gg 1. \quad (90)$$

where  $t \equiv t_2 - t_1$  corresponds the lower bound of the fitting range used in a numerical computation. For lattice data listed in table 1, fitting ranges in the four-volumes  $16^3 \times 25$ (or  $\times 33$ ) and  $24^3 \times 40$  are about  $5 \sim 9$  and  $9 \sim 13$  in lattice units, respectively [40]. As an example, for the smallest mass  $M_\pi^2 = 0.168$  in table 1 we find  $\Omega = 1.58$  for  $t = 5$ , and condition Eq. (90) is not really satisfied. For all mass values in table 1,  $\Omega$  ranges from 1.04 to 1.67. Note that in general, at sufficiently large  $M_\pi L$  and fixed  $L$  and  $t$ ,  $\Omega$  decreases as  $M_\pi$  increases. Since there are six excited states with  $|\mathbf{k}| = 2\pi/L$ , larger values of  $\Omega$  would be needed to be confident that the excited states are not contaminating the results.

### C. Relating $\langle \pi^+ \pi^0 | O_4 | K^+ \rangle$ and $\langle \bar{K}^0 | O' | K^0 \rangle$

An interesting ratio is that of  $\langle \pi^+ \pi^0 | O_4 | K^+ \rangle$  and  $\langle \bar{K}^0 | O' | K^0 \rangle$ , because it is independent of  $\alpha_{27}$  (or  $\alpha_{27}^q$  in the quenched case). We will consider the dimensionless quantity

$$\mathcal{R} = f_K \frac{\langle \pi^+ \pi^0 | O_4 | K^+ \rangle}{\langle \bar{K}^0 | O' | K^0 \rangle} \quad (91)$$

both for the physical and the unphysical case, where in the latter case the unphysical weak matrix element  $\langle \pi^+ \pi^0 | O_4 | K^+ \rangle$  is used. This ratio was examined in ref. [21] at tree-level for the physical case. We can parametrize  $\mathcal{R}$  as

$$\mathcal{R}_{phys}^f = \frac{3i}{2\sqrt{2}} \frac{m_K^2 - m_\pi^2}{m_K^2} (1 + R_{phys}) \quad (92)$$

for the physical case, and

$$\mathcal{R}_{unphys}^{f,q} = \frac{3i}{\sqrt{2}} (1 + R_{unphys}^{f,q}) \quad (93)$$

for the unphysical case (with degenerate quark masses). In these equations,  $R$  stands for one-loop contributions, *i.e.*  $R = 0$  at tree level. (Note that, at tree level there is no difference between the full and quenched theories in the unphysical case.)

At one loop, we evaluate  $R_{phys}$  again at two choices of  $\Lambda$ : 1 GeV and 770 MeV, setting  $O(p^4)$  contact terms equal to zero. Using Eqs. (7,9,30,43) we find that  $R_{phys}$  equals  $-0.94 + 0.20i$  and  $-0.62 + 0.20i$  at  $\Lambda = 1$  GeV and 770 MeV respectively. These are large corrections, and call into question the reliability of ChPT for this case.

In the unphysical (mass-degenerate) case, we find, from Eqs. (7,9,30,82),

$$\frac{\mathcal{R}_{unphys}^f}{3i/\sqrt{2}} = 1 + R_{unphys}^f = 1 + \frac{M_\pi^2}{(4\pi F_\pi)^2} \left( 3 \log \frac{M_\pi^2}{\Lambda^2} + F(M_\pi L) + P - F_1 + \frac{2}{3} (K_1 + K_2) \right) \quad (94)$$

for the full theory, and, from Eqs. (18,20,32,83),

$$\frac{\mathcal{R}_{unphys}^q}{3i/\sqrt{2}} = 1 + R_{unphys}^q = 1 + \frac{M_\pi^2}{(4\pi F_\pi)^2} \left( 3 \log \frac{M_\pi^2}{\Lambda_q^2} + F(M_\pi L) + \tilde{P} - \tilde{F}_1 + \frac{2}{3} \tilde{K} \right) \quad (95)$$

for the quenched theory. Note that the nonanalytic terms are the same in Eq. (94) and Eq. (95).

For numerical estimates of the one-loop corrections, we ignore the contact terms and set  $F_\pi = f_\pi$ , as before. Table 3 lists the resulting one-loop corrections for the same lattice data as in table 1. Both one-loop corrections in the infinite-volume limit (the chiral logarithm only),

labeled as  $R^\infty$ , and with finite-volume corrections ( $F(M_\pi L)$ ), labeled as  $R^L$ , at different cutoffs are shown.

Lattice parameters	$M_\pi^2$	$R_{(1)}^\infty$	$R_{(1)}^L$	$R_{(0.77)}^\infty$	$R_{(0.77)}^L$
$16^3 \times 25$ (or $\times 33$ )	0.168	-0.33	-0.14	-0.23	-0.039
$\beta = 5.7$ or	0.263	-0.38	-0.15	-0.23	-0.0050
$1/a = 1.0$ GeV	0.474	-0.39	-0.092	-0.12	0.18
$24^3 \times 40$	0.303	-0.39	-0.11	-0.22	0.058
$\beta = 6$ or	0.428	-0.40	-0.072	-0.15	0.17
$1/a = 1.7$ GeV					

Table 3. Nonanalytic one-loop corrections in Eq. (95) in infinite volume ( $R^\infty$ ) and in finite volume ( $R^L$ ) are shown. The subscript on  $R$  denotes  $\Lambda_q$  in GeV.  $M_\pi^2$  is in  $\text{GeV}^2$ .

Large positive finite-volume corrections partially offset the negative corrections from chiral logarithms. The uncertainties for the ratio  $\mathcal{R}_{unphys}^q$  associated with the range of cutoff explored are roughly 10% to 15% for the lower two values of  $M_\pi$ , and increase with  $M_\pi$ .

## 8. Conclusion

In this paper we have presented an analysis of the nonleptonic kaon decay mode  $K^+ \rightarrow \pi^+\pi^0$  to one loop in chiral perturbation theory, with emphasis on the comparison of results obtained from lattice QCD computations with experiment. One-loop ChPT makes it possible to gain analytic insight into three different systematic errors: quenching effects, finite-volume effects, and effects from the fact that lattice computations (so far) are at degenerate quark masses and have all external momenta vanishing. The last effect implies that on the lattice the relevant weak matrix element has been computed at an “unphysical” point. We have found that, for the most recent lattice results [1], all three effects are important.



Refs. [1,4] already employed tree-level ChPT in order to compare lattice results with experiment. At tree-level no quenching or finite-volume effects show up in ChPT, while the conversion factor between the unphysical lattice matrix element and the physical one amounts to a simple mass ratio (Eq. (85) with  $X = 1$ , or Eq. (88) with  $Y = 1$ ,  $f = f_q$  and  $\alpha_{27} = \alpha_{27}^q$ ).

This tree-level conversion factor between unphysical and physical matrix elements gets corrections at one loop, which are embodied in the one-loop correction factor  $X$  in Eq. (85).  $X$  is given by Eq. (86), which also includes finite-volume corrections. We found that, for a meson mass  $M_\pi = 0.4$  GeV and a volume  $M_\pi L = 8$ ,  $X$  is approximately 0.6, *i.e.* a substantial correction. (At  $M_\pi L = \infty$ , one finds  $X \approx 0.7$ .)

Eq. (88) gives the conversion factor between the unphysical, *quenched* matrix element in finite volume and the real-world, physical matrix element. The one-loop effects are contained in the factor  $Y$ , given in Eq. (89). Table 1 gives estimates of the factor  $Y$  for meson masses and spatial volumes used in ref. [1], while table 2 gives  $Y$  for the same masses, but in infinite volume. From a comparison of these two tables, we see that finite-volume effects cannot be ignored for these masses and volumes. In order to isolate the effect from quenching on  $Y$  we can take the ratio of  $Y$  and  $X$ . Considering only the chiral logarithms in this ratio, one finds that  $Y/X \approx 1.2$  for  $M_\pi = 0.4$  GeV,  $F_\pi = f_\pi$  and  $\Lambda = \Lambda_q = 1$  GeV (finite-volume corrections cancel between  $Y$  and  $X$ ).

In refs. [1,4], lattice results for the  $K^+ \rightarrow \pi^+\pi^0$  matrix element were corrected using tree-level ChPT, and compared with experiment. Some of the data points of ref. [1,4] are reproduced in fig. 2. In fig. 2 we also showed how the lattice points would shift, if our best estimates for the one-loop correction factor  $Y$  are included (for the error bars, see section 7). From fig. 2, we conclude that one-loop effects in ChPT narrow the gap between lattice results and the experimental value.

We should stress that there are other possible sources of discrepancy between lattice

results and the experimental value. First, in obtaining the one-loop corrected points in fig. 2, the factors  $\alpha_{27}/\alpha_{27}^q$  and  $(f_q/f)^3$  in Eq. (88) have been ignored. Since the quenched theory is different from the full theory, there is no *a priori* reason that these factors should be equal to one. Furthermore, our estimates of the factor  $Y$  have been obtained by choosing some values of the cutoff in (Q)ChPT, and ignoring all  $O(p^4)$  low-energy constants. While the error bars on our results in fig. 2 give some indication of the uncertainty introduced by this procedure, more information on these low-energy constants would be needed in order to be more confident about our estimates of  $Y$ . Third, since one-loop effects turn out to be rather substantial, one may expect that two-loop corrections cannot be completely neglected. Also, our estimate of finite-volume effects included only effects that go like inverse powers of  $L$ , and do not take into account exponential corrections. (For more detailed discussion of some of these points, see section 7.) Finally, there are possible systematic errors associated with approximations that we did not discuss at all, such as contamination of lattice results by higher excited states in Eq. (49), breaking of isospin symmetry and scaling violations. However, we believe that we have demonstrated that one-loop corrections in ChPT do move the lattice results closer to the experimental value.

If quenched lattice computations were performed with nondegenerate quark masses, this would introduce new systematic effects into the difference between lattice results and the experimental value of the  $K^+ \rightarrow \pi^+\pi^0$  matrix element, which would show up at one loop in QChPT. With nondegenerate masses, the quenched result would be dependent on the “ $\eta'$ -parameters”  $\delta$  and  $\alpha$ , and presumably it would diverge in the chiral limit (*cf.* section 6). Experience with other quantities in QChPT suggests that these new effects could be rather substantial, which would imply that nondegenerate quenched computations may be of limited value.

In section 4, we presented our one-loop calculation of the unquenched, physical  $K^+ \rightarrow \pi^+\pi^0$  matrix element with nondegenerate masses. For  $m_\pi = 0$ , our result agrees with that

of ref. [16]. However, we note that this quantity is particularly sensitive to the pion mass, so that its numerical value at the physical pion mass can deviate significantly from that at  $m_\pi = 0$ .

Finally, we reviewed and extended previous existing one-loop calculations in ChPT of the kaon B-parameter,  $B_K$  [16,36,19,29,20,5] (*cf.* section 3). We extended the quenched calculation of refs. [29,5] to include the dependence on the  $\eta'$ -parameter  $\alpha$ . Furthermore, we discussed a modified version that could be of use for staggered fermion QCD (*cf.* Appendix A). In section 7, we used our results in order to calculate a quantity which is basically the ratio of the  $K^0 - \bar{K}^0$  and  $K^+ \rightarrow \pi^+\pi^0$  matrix elements. This ratio is independent of the  $O(p^2)$  low-energy constant  $\alpha_{27}$ , and therefore is of some interest (it is not independent of  $O(p^4)$  low-energy constants). For the real world, we found that this ratio has large one-loop corrections (mostly due to large chiral logarithms in the  $K^0 - \bar{K}^0$  matrix element). For the lattice data of ref. [1] these one-loop corrections change the tree-level value by some +20 to -40 % (*cf.* table 3).

### Acknowledgements

We would like to thank Steve Sharpe, Akira Ukawa and, in particular, Claude Bernard for discussions. This work is supported in part by the US Department of Energy (MG as an Outstanding Junior Investigator).

### Appendix A: $B_K^q$ with staggered fermions

In this Appendix, we present a somewhat modified expression for  $B_K^q$  which may be relevant for quenched staggered-fermion lattice computations of this quantity at values of the lattice spacing where the continuum flavor symmetry is not yet completely restored.

It has been observed [41,42] that the double-pole contribution from the Goldstone mesons appearing on the loops in QChPT have to be (staggered-)flavor singlets, while the external mesons are usually taken to be the one exact Goldstone boson (per staggered fermion field) of staggered-fermion QCD, which is not a flavor singlet. At typical values of the lattice spacing, one observes that the nonexact Goldstone bosons are more or less degenerate [43], while their masses do not go to zero for zero quark mass, due to the staggered breaking of chiral symmetry. Of course, (Q)ChPT, being a continuum effective theory, is inherently inadequate to accommodate scaling-violation effects. However, heuristically, if we denote the masses of the nonexact Goldstone bosons as  $\overline{m}_K$  and  $\overline{m}_\pi$ ,  $B_K^q$  will depend on these nonexact Goldstone masses through the double-pole contribution to the one-loop corrections. Inserting  $\overline{m}_K$  and  $\overline{m}_\pi$  into the double-pole terms, and ignoring  $O(p^4)$  contact terms, we now get

$$\begin{aligned}
B_K^q = B^q & \left( 1 + \frac{m_K^2}{(4\pi f_q)^2} \left[ -2(3 + \epsilon^2) \log \frac{m_K^2}{\Lambda^2} - (2 + \epsilon^2) \log(1 - \epsilon^2) - 3\epsilon \log \frac{1 + \epsilon}{1 - \epsilon} \right] \right. \\
& - \delta \left[ \frac{\overline{m}_K^2}{m_K^2} \left\{ -\frac{1 - \bar{\epsilon}^2}{2\bar{\epsilon}} \log \frac{1 + \bar{\epsilon}}{1 - \bar{\epsilon}} + 1 \right\} - \frac{1}{2\bar{\epsilon}} \log \frac{1 + \bar{\epsilon}}{1 - \bar{\epsilon}} + 1 \right] \\
& + \frac{2}{3} \alpha \frac{\overline{m}_K^2}{(4\pi f_q)^2} \left[ \frac{\overline{m}_K^2}{m_K^2} \left\{ 2\bar{\epsilon}^2 \log \left( \frac{\overline{m}_K^2}{\Lambda^2} (1 - \bar{\epsilon}) \right) - \frac{1 - 3\bar{\epsilon}^2 - 2\bar{\epsilon}^3}{2\bar{\epsilon}} \log \frac{1 + \bar{\epsilon}}{1 - \bar{\epsilon}} + 1 + \bar{\epsilon}^2 \right\} \right. \\
& \left. \left. - \frac{1 - \bar{\epsilon}^2}{2\bar{\epsilon}} \log \frac{1 + \bar{\epsilon}}{1 - \bar{\epsilon}} + 1 \right] \right), \quad (96)
\end{aligned}$$

with  $\bar{\epsilon} = 1 - \overline{m}_\pi^2/\overline{m}_K^2$ . In this expression,  $m_K$  and  $\epsilon$  refer to the exact Goldstone boson masses. Note the appearance of terms that go like  $1/m_K^2$ . We should stress that this expression is heuristic, since it assumes that the only effect of nonzero lattice spacing is the appearance of nonexact Goldstone masses in the double-pole terms.

## Appendix B: Discussion of nonleading time exponentials from diagram (b)

In ref. [22] Maiani and Testa showed that, for any decay process with two identical final

pions as outgoing particles, the leading exponential time dependence for the final pions in the corresponding three-point Euclidean correlation function acquires power corrections in the special case that both pions are at rest, and when first the infinite-volume limit is taken. The leading correction comes from the sum over all excited states in Eq. (73) (*cf.* last line in that equation), which for infinite spatial volume becomes an integral. It has the form (*cf.* Eq.(10) of ref. [22])

$$e^{-2m_\pi(t_2-t_1)} \rightarrow e^{-2m_\pi(t_2-t_1)} \left( 1 - a_0^{I=2} \sqrt{\frac{m_\pi}{\pi(t_2-t_1)}} \right). \quad (97)$$

Note that the second term in Eq. (97) differs by a factor 1/2 as compared to Eq. (10) in ref. [22]. This takes into account the phase-space difference between distinct and identical pions in the final state. The parameter  $a_0^{I=2}$  is the  $I = 2$  pion-pion  $S$ -wave scattering length. Note also that  $E_{2\pi} \rightarrow 2m_\pi$  in the exponent, since this is an infinite-volume result. Indeed, if we replace the sum over  $\mathbf{k}$  in the last line of Eq. (73) by an integral, we find Eq. (97) with

$$a_0^{I=2} = -\frac{1}{8\pi} \frac{m_\pi}{f_\pi^2}, \quad (98)$$

which is the tree-level ChPT expression for the  $I = 2$   $S$ -wave scattering length. This infinite-volume result constitutes a useful check of our calculation.

### Appendix C: Finite-volume expansion of $C(m_\pi L)$ in Eq. (79)

In ref. [38] Lüscher proved that, for a function  $f$  of which all derivatives are square-integrable,

$$\sum_{\mathbf{k} \neq 0} \frac{f(\mathbf{k}^2)}{(\mathbf{k}^2)^q} \cong L^3 \frac{1}{(2q-2)!} \int \frac{d^3\mathbf{k}}{(2\pi)^3} \frac{1}{\mathbf{k}^2} (\Delta_k)^{q-1} f(\mathbf{k}^2) + \sum_{j=0}^q \left( \frac{2\pi}{L} \right)^{2(j-q)} f^{(j)}(0) z(q-j), \quad (99)$$

with integer  $q > 0$  and  $f^{(j)}(0) = \left( \frac{d}{dk^2} \right)^j f(k^2)|_{k^2=0}$ , up to corrections vanishing faster than any power of  $L^{-1}$ .  $\Delta_k$  is the Laplacian with respect to  $\mathbf{k}$  and  $z(q) = Z_{00}(q, 0)$  is a zeta function [38], with

$$z(1) = -8.91363292, \quad z(0) = -1. \quad (100)$$

For a smooth function  $g(\mathbf{k}^2)$  for which the sum in Eq. (99) is ultraviolet divergent, we introduce a regulator mass  $M$ , and apply Eq. (99) to

$$f(\mathbf{k}^2) = g(\mathbf{k}^2) \left( \frac{M^2}{\mathbf{k}^2 + M^2} \right)^n, \quad (101)$$

where the positive integer  $n$  is chosen sufficiently large to make  $f$  square-integrable. For  $M^2 \rightarrow \infty$ ,

$$f(\mathbf{k}) \longrightarrow g(\mathbf{k}), \quad (\Delta_k)^{(q-1)} f(\mathbf{k}) \longrightarrow (\Delta_k)^{(q-1)} g(\mathbf{k}) \quad \text{and} \quad f^{(j)}(0) \longrightarrow g^{(j)}(0). \quad (102)$$

We see that the finite-volume corrections in Eq. (99) are finite in the  $M^2 \rightarrow \infty$  limit, and could have been calculated directly from  $g$ , while the integral “carries” the ultraviolet divergence. Applying this to  $C(m_\pi L)$  in Eq. (79) and keeping only the universal logarithmic cutoff dependence from the integral term, we find

$$C(m_\pi L) \rightarrow \frac{3}{2(4\pi)^2} \log \frac{m_\pi^2}{\Lambda^2} - \frac{3z(1)}{8\pi^2} \frac{1}{m_\pi L} + \frac{9}{4} \frac{1}{(m_\pi L)^3}, \quad (103)$$

valid up to corrections vanishing faster than any power of  $L^{-1}$ . For a discussion of the power-like ultraviolet divergences and contact terms we refer to section 6.

## REFERENCES

1. C.W. Bernard and A. Soni, Nucl. Phys. **B17** (Proc. Suppl.), 495 (1990).
2. J.F. Donoghue, E. Golowich and B.R. Holstein, Dynamics of the Standard Model, (Cambridge, 1992); A.J. Buras, *in* Proceedings of Workshop on QCD: 20 Years Later, Aachen, Germany, edited by P.M. Zerwas and H.A. Kastrup (World Scientific, 1993); E. de Rafael, *in* CP Violation and the Limits of the Standard Model, Proceedings of 1994 TASI School, edited by J.F. Donoghue (World Scientific, 1995).
3. C.W. Bernard and A. Soni, *in* Quantum Fields on the Computer, edited by M. Creutz (World Scientific, 1992).
4. C.W. Bernard, *in* From Actions to Answers, Proceedings of the 1989 TASI School, edited by T. DeGrand and D. Toussaint (World Scientific, 1990).
5. S.R. Sharpe, *in* CP Violation and the Limits of the Standard Model, Proceedings of 1994 TASI School, edited by J.F. Donoghue (World Scientific, 1995).
6. R. Gupta and T. Bhattacharya, Nucl. Phys. **B47** (Proc. Suppl.), 473 (1996).
7. D. Pekurovsky, G. Kilcup and L. Venkataraman, hep-lat/9608134, *to be published in* Lattice '96, Proceedings of the International Symposium on Lattice Field Theory, St. Louis, U.S.A., edited by C.W. Bernard, M.F.L. Golterman, M.C. Ogilvie and J. Potvin; S. Aoki *et al.*, hep-lat/9608134, *ibid*; W. Lee and K. Klomfass, hep-lat/9608089.
8. M.B. Gavela *et al.*, Nucl. Phys. **B306**, 677 (1988).
9. C.W. Bernard and A. Soni, Nucl. Phys. **B9** (Proc. Suppl.), 155 (1989).
10. J. Gasser and H. Leutwyler, Phys. Lett. **B184**, 83 (1987); Phys. Lett. **B188**, 477 (1987); Nucl. Phys. **B307**, 763 (1988); H. Leutwyler, Nucl. Phys. **B4** (Proc. Suppl.),

- 248 (1988); Phys. Lett. **B189**, 197 (1987); H. Neuberger, Nucl. Phys. **B300**, 180 (1988); P. Hasenfratz and H. Leutwyler, Nucl. Phys. **B343**, 241 (1990).
11. C.W. Bernard and M.F.L. Golterman, Phys. Rev. **D46**, 853 (1992); Nucl. Phys. **B26** (Proc. Suppl.), 360 (1992).
  12. S.R. Sharpe, Phys. Rev. **D46**, 3146 (1992).
  13. N. Isgur, K. Maltman, J. Weinstein and T. Barnes, Phys. Rev. Lett. **64**, 161 (1990).
  14. M.B. Gavela *et al.*, Phys. Lett. **B211**, 139 (1988).
  15. J. Kambor, J. Missimer and D. Wyler, Nucl. Phys. **B346**, 17 (1990).
  16. J. Bijnens, H. Sonoda and M.B. Wise, Phys. Rev. Lett. **53**, 2367 (1984).
  17. W.A. Bardeen, A.J. Buras and J.-M. Gérard, Phys. Lett. **B192**, 138 (1987).
  18. J. Kambor, J. Missimer and D. Wyler, Phys. Lett. **B261**, 496 (1991).
  19. J. Kambor, *in* Effective Field Theories of the Standard Model, Proceedings of Workshop on Effective Field Theories, Dobogoko, Hungary, edited by U. G. Meissner (World Scientific, 1992).
  20. C. Bruno, Phys. Lett. **B320**, 135 (1994).
  21. J.F. Donoghue, E. Golowich and B.R. Holstein, Phys. Lett. **B119**, 412 (1982).
  22. L. Maiani and M. Testa, Phys. Lett. **B245**, 585 (1990).
  23. S. Weinberg, Phys. Rev. **166**, 1568 (1968); S. Coleman, J. Wess and B. Zumino, Phys. Rev. **177**, 2239 (1969); C.G. Callan, S. Coleman, J. Wess and B. Zumino, Phys. Rev. **177**, 2247 (1969).
  24. S. Weinberg, Physica **96A**, 327 (1979).



25. J. Gasser and H. Leutwyler, Nucl. Phys. **B250**, 465 (1985).
26. A. Morel, J. Physique **48**, 111 (1987).
27. S.R. Sharpe, Nucl. Phys. **B17** (Proc. Suppl.), 146 (1990).
28. C.W. Bernard and M.F.L. Golterman, Nucl. Phys. **B30** (Proc. Suppl.), 217 (1993).
29. S.R. Sharpe, Nucl. Phys. **B30** (Proc. Suppl.), 213 (1993).
30. C.W. Bernard and M.F.L. Golterman, Phys. Rev. **D53**, 476 (1996); Nucl. Phys. **B46** (Proc. Suppl.), 553 (1996).
31. M.J. Booth, Phys. Rev. **D51**, 2338 (1995); hep-lat/9412228.
32. S.R. Sharpe and Y. Zhang, Phys. Rev. **D53**, 5125 (1996).
33. G. Ecker, J. Gasser, A. Pich and E. de Rafael, Nucl. Phys. **B321**, 311 (1989).
34. A. Pich and E. de Rafael, Nucl. Phys. **B358**, 311 (1991); C. Bruno and J. Prades, Z. Phys. **C57**, 585 (1993).
35. M.F.L. Golterman, Acta Phys. Polonica **B25**, 1731 (1994).
36. W.A. Bardeen, A.J. Buras and J.-M. Gérard, Phys. Lett. **B211**, 343 (1988).
37. H.W. Hamber, E. Marinari, G. Parisi and C. Rebbi, Nucl. Phys. **B225** [FS9], 475 (1983); G. Parisi, Phys. Rep. **103**, 203 (1984).
38. M. Lüscher, Comm. Math. Phys. **105**, 153 (1986).
39. H. Georgi, Weak Interactions and Modern Particle Theory (Benjamin, 1984).
40. C.W. Bernard (private communication).
41. R. Gupta, Nucl. Phys. **B42** (Proc. Suppl.), 85 (1995).

42. S.R. Sharpe, hep-lat/9609029, *to be published in* Lattice '96, Proceedings of the International Symposium on Lattice Field Theory, St. Louis, U.S.A., edited by C.W. Bernard, M.F.L. Golterman, M.C. Ogilvie and J. Potvin.
43. N. Ishizuka, M. Fukugita, H. Mino, M. Okawa, A. Ukawa, Nucl. Phys. **B411**, 875 (1994).